INFORMATION TO USERS

This was produced from a copy of a document sent to us for microfilming. While the most advanced technological means to photograph and reproduce this document have been used, the quality is heavily dependent upon the quality of the material submitted.

The following explanation of techniques is provided to help you understand markings or notations which may appear on this reproduction.

1. The sign or "target" for pages apparently lacking from the document photographed is "Missing Page(s)". If it was possible to obtain the missing page(s) or section, they are spliced into the film along with adjacent pages. This may have necessitated cutting through an image and duplicating adjacent pages to assure you of complete continuity.

2. When an image on the film is obliterated with a round black mark it is an indication that the film inspector noticed either blurred copy because of movement during exposure, or duplicate copy. Unless we meant to delete copyrighted materials that should not have been filmed, you will find a good image of the page in the adjacent frame.

3. When a map, drawing or chart, etc., is part of the material being photographed the photographer has followed a definite method in "sectioning" the material. It is customary to begin filming at the upper left hand corner of a large sheet and to continue from left to right in equal sections with small overlaps. If necessary, sectioning is continued again—beginning below the first row and continuing on until complete.

4. For any illustrations that cannot be reproduced satisfactorily by xerography, photographic prints can be purchased at additional cost and tipped into your xerographic copy. Requests can be made to our Dissertations Customer Services Department.

5. Some pages in any document may have indistinct print. In all cases we have filmed the best available copy.

University
Microfilms
International

300 N. ZEEB ROAD, ANN ARBOR, MI 48106
18 BEDFORD ROW, LONDON WC1R 4EJ, ENGLAND

Downloaded from SHAREOK. Persistent Handle URL: https://hdl.handle.net/11244/4728

8018931

MOUSSA, MOHAMED MAHMOUD

NEW TECHNIQUES TO MEASURE AND CONTROL CORROSION OF DRILLING FLUIDS AT ELEVATED TEMPERATURE

The University of Oklahoma PH.D. 1980

University Microfilms International 300 N. Zeeb Road, Ann Arbor, MI 48106 18 Bedford Row, London WC1R 4EJ, England

PLEASE NOTE:

In all cases this material has been filmed in the best possible way from the available copy. Problems encountered with this document have been identified here with a check mark ✓.

1. Glossy photographs _____
2. Colored illustrations _____
3. Photographs with dark background ✓
4. Illustrations are poor copy ✓
5. Print shows through as there is text on both sides of page _____
6. Indistinct, broken or small print on several pages _____ throughout _____
7. Tightly bound copy with print lost in spine _____
8. Computer printout pages with indistinct print _____
9. Page(s) _____ lacking when material received, and not available from school or author _____
10. Page(s) _____ seem to be missing in numbering only as text follows _____
11. Poor carbon copy _____
12. Not original copy, several pages with blurred type _____
13. Appendix pages are poor copy _____
14. Original copy with light type _____
15. Curling and wrinkled pages _____
16. Other _____

University Microfilms International

THE UNIVERSITY OF OKLAHOMA

GRADUATE COLLEGE

NEW TECHNIQUES TO MEASURE AND CONTROL CORROSION OF DRILLING FLUIDS AT ELEVATED TEMPERATURE

A DISSERTATION

SUBMITTED TO THE GRADUATE FACULTY

in partial fulfillment of the requirements for the degree of

DOCTOR OF PHILOSOPHY

BY

MOHAMED MAHMOUD MOUSSA

Norman, Oklahoma

1980

NEW TECHNIQUES TO MEASURE AND CONTROL CORROSION
OF DRILLING FLUIDS AT ELEVATED TEMPERATURES

APPROVED BY

DISSERTATION COMMITTEE

ACKNOWLEDGEMENTS

The author wishes to express his sincere appreciation for the constructive guidance and encouragement of Dr. Djebbar Tiab, School of Petroleum and Geological Engineering, University of Oklahoma, under whose supervision this study was completed.

Appreciation is expressed to the PGE management and their support in building the PGE loop to complete this research. Also, appreciation is expressed to Mr. N. Knight for his technical help.

Acknowledgement is also made to the Sandia Laboratory and DOE for the financial support which made this research possible.

TABLE OF CONTENTS

Page

ACKNOWLEDGEMENTS iii

LIST OF TABLES vi

LIST OF ILLUSTRATIONS viii

ABSTRACT x

Chapter

I. INTRODUCTION 1

1.1 Statement of the Problem 4
1.2 Objectives 6
1.3 Organization of the Study 7

II. DRILLING FLUIDS AND CORROSION 11

2.1 Drilling Fluids 11
2.2 Function of the Mud Components 14
2.3 Corrosion 15

III. CORROSION THEORY 18

3.1 Electrochemical Theory 18
3.2 Chemical Theory 23
3.3 Effect of Salts on Steel Corrosion . . . 26
3.4 Factors Controlling Corrosion in Drilling Operations 29

3.4.1 Acid Gases 29
3.4.2 Velocity 31

3.5 Methods of Preventing Corrosion 33
3.6 The Economic Potential of Corrosion and Corrosion Research 35

Chapter Page

IV. EXPERIMENTAL DESIGN 37

4.1 Flow Loop Corrosion Test 37

4.1.1 Sandia-Lab Flow Loop 37
4.1.2 PGE Flow Loop 38
4.1.3 Correlation Between the Two Loops. 47

4.2 Rolling Technique 48
4.3 Static Technique 49
4.4 Pressure Transducer Calibration 52

4.4.1 Equipment Zero Process 52

4.4.1.1 Pressure Transducer (DP-15-3000 psia) absolute 52
4.4.1.2 Pressure Differential Transducer (DP-15 ± 50) . 53

4.4.2 Equipment Readings 53

V. TEST PROCEDURE 55

5.1 Mud Preparation 55
5.2 Corrosion Test (Flow Loop) 56
5.3 Test Duration 57
5.4 Pump Maintenance 58
5.5 Test Specimen 59
5.6 Number of Specimens 60
5.7 The Sample Preparation 60

VI. ANALYSIS OF TEST RESULTS 62

VII. CONCLUSIONS AND RECOMMENDATIONS FOR FUTURE RESEARCH 72

7.1 Conclusions 72
7.2 Recommendations for Future Research . . . 73

REFERENCES 76

APPENDICES

A. Formulae Used 79
B. Tables and Illustrations 82
C. Set-Up Photographs 142

LIST OF TABLES

Table		Page
1.	Corrosion, Rolling, Saline Commercial Mud . . .	84
2.	Corrosion, Rolling, Polymer Mud	86
3.	Corrosion, Rolling, A-RB1-200	88
4.	Corrosion, Rolling, A-RB1-300	89
5.	Corrosion, Rolling, A-RB1-400	90
6.	Corrosion, Rolling, A-RB1-500	91
7.	Corrosion, Rolling, C-RB1-200	92
8.	Corrosion, Rolling, C-RB1-300	93
9.	Corrosion, Rolling, C-RB1-400	94
10.	Corrosion, Rolling, C-RB1-500	95
11.	Summary of the Rolling Test Results	96
12.	Stability Test, Sandia-Lab Flow Loop	99
13.	Corrosion Test, Sandia-Lab Flow Loop, Tap Water, 24 hours Aging	100
14.	Corrosion, Rolling, Aging Time 24 hours	101
15.	Corrosion, Flow Loop, Distilled Water, No Aging	102
16.	Corrosion, Rolling, Distilled Water, No Aging .	103
17.	Corrosion, Sandia-Lab Flow Loop, Mud B_1	108
18.	Corrosion, Rolling, Mud B_1	109
19.	Corrosion, PGE Flow Loop, Mud B_1	110
20.	Rheological and Stabilization Test, B_1	113

Table		Page
21.	Corrosion, Sandia-Lab Flow Loop, Mud B_1	114
22.	Corrosion, Rolling, Mud B_1	114
23.	Static Corrosion Test, Mud B_1	115
24.	Rheological Data	116
25.	Corrosion, Rolling, A-RB2-200	120
26.	Corrosion, Rolling, A-RB2-300	120
27.	Corrosion, Rolling, A-RB2-400	121
28.	Corrosion, Rolling, A-RB2-500	121
29.	Static Test, Mud Type B_2	124
30.	Corrosion, Rolling, C-RB3-200	126
31.	Corrosion, Rolling, C-RB3-300	126
32.	Corrosion, Rolling, C-RB3-400	127
33.	Corrosion, Rolling, C-RB3-500	127
34.	Stabilization Test, Sandia-Lab Flow Loop, Mud B_3	132
35.	Corrosion Test, Sandia-Lab Flow Loop, Mud B_3	133
36.	Rheological Data with Temperature	134
37.	Stabilization, Sandia-Lab Flow Loop, Mud B_3	137
38.	Corrosion, Sandia-Lab Flow Loop, Mud B_3	138
39.	Stabilization, PGE Flow Loop, Baroid	140

LIST OF ILLUSTRATIONS

Figure		Page
1.	Galvanic or electromotive series of metals . . .	20
2.	The corrosion mechanism on iron pipe walls . . .	21
3.	Effect of NaCl concentration on corrosion of iron in aerated solution at room temperatures	28
4.	Schematic diagram of the dynamic corrosion test PGE flow loop (closed system)	39
5.	Shear Valve	41
6a.	The hydraulic system of the transducers	42
6b.	Pressure transducer DP-15 assembly	43
6c.	Pressure transducer DP-15 cross section	43
7.	Mag-corrosion cell	44
8.	Mag-corrosion cell parts	45
9.	Baroid rolling oven with the cells	50
10.	Rolling technique corrosion cell	51
11.	Corrosion rate as a function of temperature for mud B_1, constant pH, cell A	97
12.	Corrosion rate as a function of temperature for mud B_1, constant pH, cell C	98
13.	Bar diagram, corrosion rate vs. temperature (tap water, aged 24 hrs, temperature raised directly 400, 450°F)	104
14.	Bar diagram, corrosion rate vs. temperature (distilled water, no aging, and gradual change in temperature)	104

Figure Page

15. Bar diagram, correlation between two techniques, flow loop and rolling 105

16. Effect of temperature on pH for drilling fluid . 107

17. Bar diagram to show equal efficiency between PGE and Sandia-Lab flow loops to measure the corrosion rate 111

18. Combination of the two techniques (flow loop and rolling) 112

19. Effect of temperature on plastic viscosity, cp, and flow rate, cc/sec 117

20. Bar diagram to show the relationship between corrosion techniques (flow loop, rolling and static) 118

21. Corrosion rate vs. temperature, °F, and pH for mud B_2 123

22. Corrosion rate vs. temperature and pH for mud B_3 130

23. Corrosion rate measured by the flow loop, 1% sea salt (cold, hot linear, hot mag) 135

24. Corrosion rate for different types of flow . . . 139

25. View of the linear corrosion cell in parts loaded with the specimen 143

26. View of the flow loop, pH meter, transducers, and power switch 144

27. View of the two shear valves installed in series with the cold end of the loop 145

28. View of the linear corrosion cell attached to the cold end of the flow loop 146

29. View of the mag-corrosion and the linear cells attached to the hot end of the loop 147

30. Steam leak due to thermal cracking of one of the flow lines 148

ABSTRACT

Problems associated with geothermals and deep well drilling can be minimized by the proper choice and control of the drilling fluid formulation. High bottomhole temperature gellation of conventional muds has been avoided by employing the sepiolite (sea mud) systems. Sepiolite is a fibrous, magnesium-rich clay mineral. Several formulations of muds are tested at elevated temperature ranges from room temperature to 500°F. Also, the pH value, flow rate and pressure were changed to examine their effect on mud stability. The drilling operation is simulated in the laboratory by two flow loops.

The corrosion rate is measured under the above conditions by the weight loss technique. The corrosion cells are loaded with two flat coupons in each cell. Mild steel (1018) specimens are immersed in the drilling fluids under different types of fluid regimes. The weight loss of the specimen before and after the run during a certain period of time is a measure of the corrosion rate. The corrosion rate is minimized by adjusting the pH value and the formulation of the fluid by adding caustic soda when necessary. Corrosion rates are measured using different techniques--the flow loop, rolling and static. A new mag-corrosion

cell has been incorporated in the loop to combine the rotational motion and the linear flow of the fluids, simulating the bottomhole conditions. Correlations between techniques under different conditions are included. The corrosion rate measured by the flow loops was a result of exposing the specimens at two different temperatures (hot and cold). During the test period, the coupons experience the change in temperature from room temperature up to 450°F. Thus, the corrosion rate measured is due to the change of temperature from room temperature to the maximum in the test time.

In the rolling and static techniques, the corrosion rate is measured due to the effect of each temperature and time of exposure separately.

Corrosion is higher when using the mag-corrosion cell than when using the linear flow when both are exposed under the same conditons. Static technique rates are less than rolling. Critical pH values are determined for specific drilling fluids.

NEW TECHNIQUES TO MEASURE AND CONTROL CORROSION OF DRILLING FLUIDS AT ELEVATED TEMPERATURE

CHAPTER I

INTRODUCTION

Corrosion problems are being recognized by a larger segment of the oil well drilling, production, and refinery industry than ever before because of the complicated problems of the very deep and geothermal wells. These wells require heavy-weight, highly-treated drilling fluids. Thus, the corrosion problem must be reckoned with in the successful drilling and completing of an oil or gas well. Corrosion is an electro-chemical and surface phenomenon and invariably requires the presence of moisture and some other corrosive agents to be more active, causing considerable problems in the oil industry and others.

The higher weight, low solids water-base muds aggravate the corrosion problem in the presence of the corrosive environment, although they offer many benefits in penetration rates. Mud workover completion fluids, or packer fluids, which are chemically strong electrolytes, conduct electric current and set up a potential exchange between the anode and cathode on the drill pipe, drill collars or

casing. Acid-forming gases, carbon dioxide and hydrogen sulfide, are serious environmental corrosion accelerators that must be dealt with in drilling fluids. These are often associated with the hydrocarbons of the produced crude oil or gas as well as in formation water and are a major cause of corrosion in the petroleum industry. Acid gas contamination has resulted from drilling fluid materials that have been altered by temperature,[1,2] microbiological activity or electrochemical effects.[3] Contamination originating from thermal breakdown of drilling fluid additives is conditioned by time and temperature. Serious breakdown of many commonly used organic materials containing carbonyl or sulfur-oxygen groups into carbon dioxide or hydrogen sulfide begins approximately at 150°C (300°F). Thermally stable materials should be used when well temperatures are expected to exceed the 300°F range for extended periods because thermal degradation tends to destroy drilling fluid properties.

Microorganisms readily attack drilling fluid additives, resulting in their chemical breakdown to carbon dioxide, hydrogen sulfide and other degradation products. The breakdown of these additives can result in detrimental changes which are significant in controlling fluid properties and corrosion. Drilling fluids also contain materials that can be biodegraded into corrosion accelerators with a little effect on hydraulic properties. Practical control of microorganisms can be accomplished if pH can be maintained above 10 or if the fluid is saturated with a salt such as sodium

chloride. However, because of the proliferous nature of microorganisms in certain drilling fluids, biocides are needed for control. Chlorinated phenols or paraformaldehyde at concentrations up to 2 lb/bbl are used in drilling fluids. These treatments can vary because solids in drilling fluids usually favor the growth of microorganisms and tend to reduce the biocidal efficiency.

In an electrochemical sense, one form of corrosion by-product has been attributed to the flow of direct current in the corrosion cell. Electrochemical reduction of sulfur-oxygen groups results in hydrogen sulfide being formed at the cathode.[3] This well-known corrosion cell reaction provides reactive hydrogen near the metal cathode surface. The hydrogen combines with the ever-present sulfur-containing compounds in drilling fluid to form hydrogen sulfide which in turn will attack the steel. With properly designed control and pre-calculated programs--either chemical treatment to the bulk medium or more advanced material testing procedures, i.e., metallurgical tests--it becomes possible to avoid the corrosion damage and save $70 billion or 4% of the Gross National Product of the United States.[4]

Thus, the corrosion rate should be monitored totally using weight loss, or instantaneously using an electronic probe system; and treatment should start promptly to correct or avoid undesirable trends in the field before extensive damage occurs. The corrosion rate of any fluid is dependent on the amount of dissolved gasses (oxygen, carbon dioxide,

and hydrogen sulfide) in the drilling mud, the pH value, environment temperature and pressure, and the flow velocity.

An accurate monitoring technique, either instantaneously or totally, of the corrosion rate is necessary to select and evaluate the desirable inhibitor for each field case. An inhibitor is a substance, organic or inorganic, which, when added in small concentrations to an environment, decreases the corrosion rate. In a sense, an inhibitor can be considered as a retarding catalyst. There are numerous inhibitor types and compositions. Most of these have been developed by experimentation, and many inhibitors are proprietary in nature so that their composition is not disclosed.

1.1 Statement of the Problem

Thousands of corrosion tests are made every year to reduce the cost of corrosion. The value and reliability of the data obtained depend on details involved. Controlling and manipulating all the rate factors affecting corrosion in a particular plant or field operation is very difficult. Simulating actual drilling operations in a laboratory test is of considerable importance in obtaining reliable and reproducible results.

It is necessary to conduct a number of laboratory tests with drilling fluids of different formulations. These tests were studied in two phases.

Phase I - Stability of the drilling fluids

Under the effect of elevated temperature and pressure, fluids may suffer thermal degradation and a high tendency to gelation. The drilling fluid at this point will fail to perform well in the drilling operation. Thus, it is necessary to apply these conditions on different formulations to evaluate their effect.

Phase II - Corrosion Test using the weight loss method.

The necessary characteristics of the drilling fluid can be varied in the following ways under controlled test conditions:

1. Composition of the environment (mud formulation), i.e., types of clay, salinity, chemical additives, etc.
2. Condition of immersion, that is (i) A stationary specimen with the fluid flowing linearly and rotationally (small loop); (ii) rolling (specimen and fluid are both rotating), (this technique simulates the actual rotating drill pipe and the fluid at any particular depth in a drilling operation); (iii) static condition, which indicates the travelling period (drill bit change), fishing operations, etc.
3. Volume of test solution
4. Length of exposure in hours
5. Test temperature and thermal stability
6. Acidity or pH of the test solution
7. Heterogeneity of the solution

These factors can be combined in a proper manner to measure

the corrosion rate of the formulated drilling fluid under the various conditions and by different techniques.

It is well known that laboratory tests are characterized by small specimens and small volumes of mud solutions, but the actual conditions are simulated insofar as conveniently possible. Generally, the mud volume was the greatest problem in our tests because insufficient volume can lead to exhaustion of the corrosive constituents and give lower corrosion rates than would have occurred if the corrosive concentration were maintained. We used 250 cm^3 fluid for each square inch of specimen area.

To study the effect of temperature on corrosion of the drilling fluid using any of these techniques, the exposure time must be long enough to obtain reliable results. The temperature was increased in steps of 100°F from room temperature to 200°F, 300°F, 400°F and, in some cases, to 500°F.

1.2 Objectives

1. The first objective was to design an adequate experimental technique to measure the corrosion rate by the weight loss method under field conditions. It is impossible to simulate the actual field operations of pressure, temperature, fluid rotation, drill pipe and drill bit rotation, shearing, fluid contamination, acid-gas intrusion, and depth scaling. However, the study here covers two important techniques, linear (flow loop) and rotational (rolling), in detail.

2. From the experiment it is possible to obtain information on the interrelation between the corrosion results collected from all techniques and operating variables to help in the diagnosis of the problem. This information is also very useful for improved control of corrosion and more efficient drilling operations.

1.3 Organization of the Study

The experimental study was actually divided into three categories:

Category I: Mud Formulation and Preparation

This category covers the preparation of different batches of commercial and geothermal water-base mud. The percentage of each component is varied to meet a specific desirable characteristic in the formulated drilling fluid. The fluid is mixed in the laboratory by the magcobar multimixer for a period of time long enough to assure clay hydration and uniform distribution of each component in the suspension.

Rheological properties of the mud such as plastic viscosity, cp, yield point, gell strength, lb/100 ft^2, were measured just prior to each test either dynamically or statically by the Baroid V.G. Rheometer.

Category II: Stability Test Using the Flow Loop

The stability test measures the ability of a particular drilling fluid to stand such severe conditions of temperature and pressure. The mud was circulated from the

reservoir at room temperature through the flow lines, heated up to the desired temperature while passing the test section, then back to the reservoir. The fluid is driven by a pump system at a constant flow rate simulating the actual field operation in which the drilling fluid is pumped through the drill pipe from the surface downhole, experiencing the bottom-hole pressure and temperature, then back to the surface through the annular space.

For the purpose of the test, the stability was determined by measuring the pressure differential of the transducers across the test sections every 15 minutes. If the readings were very close, this would indicate that the viscosity of the fluid was about equal despite changing the temperature of the system in a certain period of time. In this study, system failure is defined as the moment at which any reading obtained is in a range from 6 to 10 times the same reading at room temperature. At this moment the system must be shut off, and the run terminated. Plugging of the lines, especially in higher temperature runs (above 400°F), was mainly due to the gellation tendency of the bentonite clay and was a problem. The tests had to be terminated several times.

Category III: Corrosion Test

The method described in this study is intended primarily to monitor the corrosion rates for a group of drilling fluids formulated to be more convenient and non-corrosive for geothermals and deep wells having temperatures greater

than 400°F. Three techniques were used to obtain accurate data under the bottomhole conditions using the weight loss method. This method estimates the corrosion rate (mpy) as a function of weight loss (before and after the run) in milligrams, surface area of the specimen (square inches) immersed in the medium, and the time of exposure in hours. The size of the coupons was 1/2 x 2•1/2 x 1/16. A rectangular flat shape was chosen to suit the needs of the test purpose and NACE and ASTM standards.

An adequate specimen holder, made from a corrosion and electrically resistant material, was fabricated to hold it firmly in the housing without any galvanic effects between the coupons and the cell. The specimen holder was oriented in a vertical position; and the distance between the two installed coupons was wide enough to permit good contact between the electrolyte and the coupon surface and uniform flow velocity, which is dependent on the pump capacity in the system.

The test duration of the flow loop was limited and dependent on the system efficiency, such as pumps, heaters, transducers, etc. Corrosion rate data obtained from the flow loops were a result of exposing the specimen to the medium and changing the system temperature periodically in steps of 100°F up to 400 and 480°F maximum. The time of exposure also includes the time taken to cool the system off by flushing it with water until room temperature was reached again.

In the rolling technique, however, the specimen used was taken out after each run at one temperature and cleaned, reweighed and put back in the cell again, ready for the new run at a higher temperature. The temperature values applied were 200, 300, 400, 500°F, and the test duration ranged from 20 to 24 hours. Thus, the corrosion rates measured by the rolling technique are obtained at each temperature, using two corrosion cells for one fluid. The drilling fluid which contains sepiolite and resinex material stayed in a liquid phase in good shape at elevated temperatures (500°F) with no dangerous gellation. However, the other commercial drilling fluids were almost cooked. A very strong, hydrogen sulfide odor was detected at 400°F due to the thermal cracking of the sulfonate group of the resinex. Consequently, the corrosion rate increased, especially when the pH was low in the medium.

In the static technique, the cells were loaded with the test fluid and the specimens, then set on a shelf for two weeks at room temperature. Elevated temperatures were also used. The test was run at different pH values. The purpose was to simulate the field operation under static conditions, for instance, changing the drill bit or fishing some drilling tools from the bottom of the hole.

CHAPTER II

DRILLING FLUIDS AND CORROSION

2.1 Drilling Fluids

The rotary system of drilling requires the circulation of a drilling fluid (mud) from the surface to downhole through a big system of rig pumps. From the suction side of this pump the mud passes through the pump and surface piping in the drill pipe. It then passes through the internal part of the drill pipe and flows through the drill bit nozzles, where prevailing severe conditions in the vicinity of the drill bit (i.e., high pressure and high temperature) are encountered. The drilling fluid then returns to the surface through the annulus between the drill pipe and the wall of the hole inside the open hole and/or cased section, carrying the cuttings from the bottom to the surface and keeping the hole clean. At this point, when it reaches the flow lines, it usually passes over a shaker screen system to remove the well bore cuttings from the fluid. Once again on the surface, the mud returns to the prevailing conditions of the surface (atmospheric pressure, surface temperature and no shear). In addition to the changes in temperature and pressure, the shearing in the vicinity of the bottom hole must be included. This is mainly nozzle shear due to

the jet flow and rotation stress due to the high speed of the drill bit.

Before being recirculated downhole the fluid may be processed by means of special solids-handling equipment or chemically treated due to the composition alteration of the drilling fluid. The drilling fluid alteration is usually due to the following reasons:

1. The intrusion of the acid gases from the drilled formation into the circulated fluid. These gases are hydrogen sulfide (H_2S) and/or carbon dioxide (CO_2).

2. Salt contamination when drilling anhydrite or salt domes, formation water. These salts are KCl, NaCl, $CaCl_2$, $MgCl_2$, etc.

3. Surface areation due to continuous exposure to the surface.

4. Filtration loss into the permeable formation which might change the mud density. This phenomenon usually occurs when a considerable difference exists between the formation pressure and the hydrostatic pressure at a certain point in the hole. The filtration rate increases as the differential pressure increases and the formation permeability at that point increases.

5. Thermal degradation of the drilling fluids at the bottom hole due to severe conditions of high temperature and pressure.

There are many types of drilling fluids or muds. They usually are named according to the continuous phase,[5]

water, oil or gas, and the type of chemical inhibited for certain desired performance characteristics. One of the most important facts to consider is that drilling fluid systems are large volume, high temperature, high pressure, and dynamic systems. The density ranges from about 8.3 ppg to about 21 ppg in certain cases. The pH of water-base muds may range from a low of 6 to over 13. The chloride content may range from less than 100 mg/l to saturation of approximately 190,000 mg/l chloride ions. Soluble calcium and magnesium ions may be present from a trace to a range of 50,000 mg/l in some special cases. Sulfates and bicarbonates are present. Sulfides may be formulated from the gas acids. Actually, they can be derived from several sources, including make-up water or drilling into a formation containing sour gas.

Water-base muds refer to those drilling fluids which contain in suspension clays and other solids in water (fresh or salt) as a continuous phase. Oil-base muds are suspensions of solids in oil. High flash-point diesel oils are commonly used as the liquid phase, and the necessary finely dispersed solid is oxidized (air-blown) asphalt. Barite and galina are used as weighting materials to increase the density. Oil-base muds are used for such special purposes as preventing the caving of certain shales and particularly as completion muds for drilling into sensitive sands which are damaged by water.

Water-in-oil-emulsion muds have been developed principlly for well completion purposes. In these fluids, oil is the continuous phase and water is in the form of small droplets. They are referred to as inverted emulsion muds. Special soaps and surfactants are required in their preparation as emulsifying agents. A combination of fluid streams has been used successfully where compressed air is pumped into the drill string along with the regular drilling fluid.

2.2 Functions of Mud Components

(a) Bentonite Clay

Bentonite is a plastic colloidal clay largely made up of the mineral sodium montmorillonite, a hydrated aluminum silicate of extremely fine and variable particle size. They are formed of alternate sheets of silica and alumina, with slightly different arrangements to make up unit layers of each of the clay minerals. For use in drilling fluids, bentonite has a yield in excess of 85 bbl/ton of 15 centipoise (cps) mud.

(b) Sepiolite Clay

Sepiolite is a fibrous, magnesium-rich clay mineral with a structure similar to attapulgite clay. In contrast to attapulgite, sepiolite also provides (1) some fluid-loss control, (2) reduction of lost circulation, (3) prevention of high bottomhole temperature gelation of conventional bentonite systems.[6]

Sepiolite clay is extremely stable at elevated temperatures. The combination of sepiolite and bentonite with the right proportions will improve the fluid stability and the desirable characteristics to withstand such severe conditions in drilling. Data from 10 wells drilled in southern California's Imperial Valley area indicate that sepiolite provides better thermal stability than other clays in environments with temperatures exceeding 400°F.

2.3 Corrosion

Metal tools were used in drilling operations as early as 256 B.C.[7] Ancient well drillers were interested in obtaining fresh water or brine and considered oil seeping into the well bore highly annoying. Although little has been recorded about corrosion problems in the early days of the petroleum industry, the existence of this problem is certainly indicated by records showing that as early as 1825 special fishing tools were used to retrieve drilling equipment that broke off in the hole.

Equipment failures were once generally regarded as purely mechanical problems. Today, corrosion is clearly understood as a major cause of drilling equipment failure. More than fifty years ago, serious attention was given to mitigating corrosion in drilling and packer fluids. Swan[8] was granted a patent in 1919 on the use of an anti-corrosive, viscous, tar oil for drilling and packer fluids. This simple approach was the predecessor of the highly efficient oil-base

and oil-emulsion fluids in use today. One of the first studies on the use of corrosion inhibitors in drilling fluid was published by Speller.[9] Speller's approach was unique. He determined that suspended colloids (bentonite) would reduce oxygen corrosion. Colloidal particles were used to interfere with the diffusion of oxygen to the metal surface.

Laboratory studies in 1936 evaluated sodium sulfite and quebracho extracts as oxygen scavengers in drilling fluids. The two materials were reported to be substantially equal in removing oxygen, the quebracho had other beneficial effects on mud properties. It has been extensively used in drilling fluids for rheological control with little attention to its oxygen scavenging ability. There is evidence now that catalyzed sodium sulfite will remove oxygen at a much faster rate than will quebracho.

An early organized study of corrosion behavior was first sponsored by the American Association of Oil Well Drilling Contractors in 1946. In this study McMaster[9] tested sodium chromate and sodium hydroxide as inhibitors. Betz[10] also proposed the use of sodium chromate to inhibit drill pipe corrosion and suggested the possible use of sodium nitrite for the same purpose. Historically, control of drilling corrosion was primarily concerned with oxygen contamination. Chemical treatments were used to scavenge oxygen, interfere with oxygen diffusion or passivate the metal by using oxidizing material.

Early studies also investigated different types of corrosion failures. Thomas[11] and Grant[12] did good work on the cause and prevention of drill-pipe and tool-joint troubles. Maradudin[13] discussed the failure modes, including sulfide stress corrosion cracking (SSCC) of drill pipe and tubular goods. However, current research and practice in drilling fluid corrosion control considers all the known possible contaminants, i.e., acid gases (H_2S and CO_2) and oxygen (O_2), and all types of equipment failure. Bush[14] outlined current methods to detect corrosion contaminants and described techniques using cationie, amine inhibitors. Behrens[14] reported on a technique employing downhole corrosion coupons to measure the corrosion rate of drill pipe using a specific drilling fluid.

Bush developed a test to evaluate hydrogen embrittlement tendencies. These tools are frequently used to estimate the rate and type of corrosion attach and evaluate the effectiveness of inhibition techniques. Corrosion mitigation during drilling has been the object of contributions from many sources, but corrosion problems do not stop when the total depth of the well is reached.

J. Perkins and others[15] developed a "circling-foil" apparatus to study velocity effects on corrosion processes. The design was used initially to expose single metals and galvanic couples of some common marine structural materials in a sea water electrolyte under controlled velocity up to 3 m/s relative velocity.

CHAPTER III

CORROSION THEORY

3.1 Electrochemical Theory

Most corrosion specialists describe the corrosion mechanism as an electrochemical process[13] as a result of observations on the behavior of iron in aqueous media. This mechanism, now with overwhelming evidence in its support, showed that corrosion of metals is largely accomplished by the action of a network of short-circuited electrolyte cells in an amount chemically equivalent to the reaction at the cathodes.

For this process to occur, three requirements must be fulfilled.

1. An electromotive force or potential difference must be present. Before a metal can corrode, it must have an anode or area that has a positive potential which attracts negatively charged particles or ions (anions), and a cathode or area that has a negative charge or potential to which positively charged particles or ions (cations) are attracted.

2. There must be an electrical circuit or couple established between the anode and the cathode.

3. The anode and cathode, electrically connected, must be in contact with a solution that will conduct a current (electrolyte). Water containing dissolved salts serves this need.

For the first criterion, every new piece of oilfield iron product--whether it be tubular goods (drill pipes, casing, tubing, drill collars), pumps, rods, pressure vessels, etc.--contain anodic and cathodic areas. Normalizing or heat treating may reduce these areas a little, but some always remain. The use of dissimilar metals is still another common occurrence of "built-in" anodes and cathodes. Generally, metals or alloys at the top of the electromotive or galvanic series (Fig. 1) are corroded when coupled to metals below them--providing the other requirements for corrosion are met.

Of course, the second criterion for corrosion is practically met in most drilling operations, oil producing or water injection equipment because differences in potential may be found in the same section of metal or in different parts installed in intimate contact with each other. To transport a fluid from the surface to downhole, to conduct a water-injection program--any of these fluids necessitates that much of the equipment used come in contact with some water, which satisfies the third criterion.

The corrosion phenomenon under the presence of these factors can be discussed using the diagram of Fig. 2 as follows. On a drill pipe there is an anode and a cathode; the metal at the anode loses two electrons which flow through

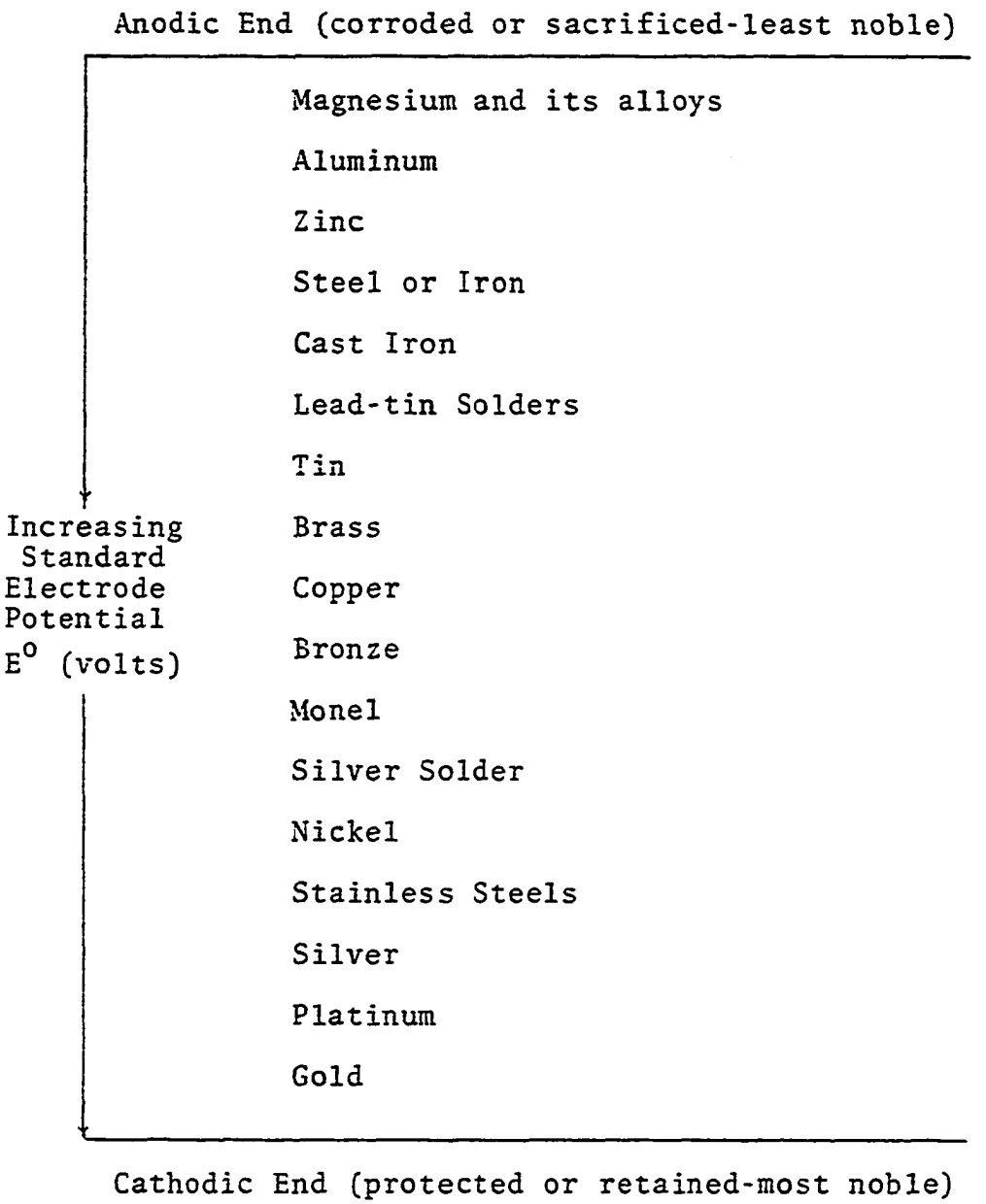


FIGURE 1: Galvanic or electromotive series of metals.

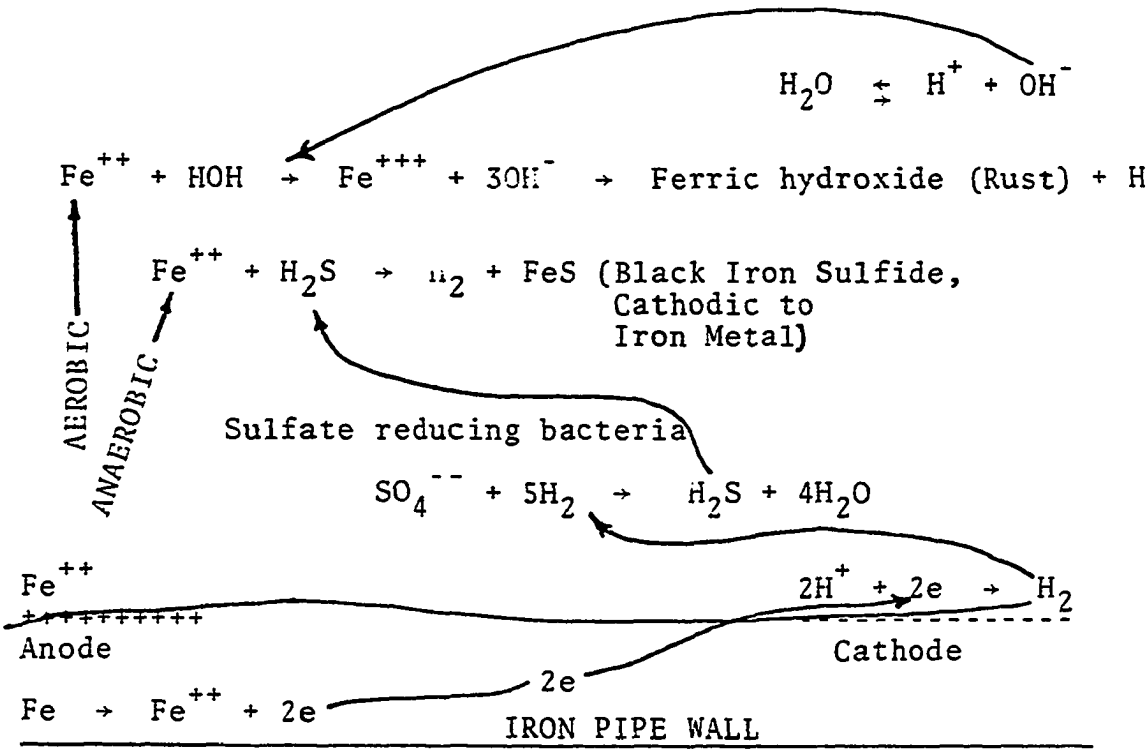


FIGURE 2: For corrosion to proceed the cathode must be depolarized, and sulfate-reducing bacteria can accomplish this as shown. The cathode may also be depolarized if oxygen is present and it reacts with hydrogen at the cathode, or if the pH is low and hydrogen gas is evolved at the cathode. (The last two reactions are not shown.)[18]

the metal pipe to the cathode. Induced current will flow in the opposite direction and may be thought of as passing through the electrolyte. The surface reaction is as follows:

$$Fe \rightarrow Fe^{++} + 2e^{-}$$

The rate of this reaction is found to be dependent upon the rate of the cathode reaction; hence, the corrosion rate is "cathodically controlled." The iron ion, Fe^{++}, enters the solution as a positively-charge soluble particle of iron. The cathode, being negatively charged, attracts hydrogen ions (H^{+}) which arise from the disassociation or ionization of water.

$$H_2O \rightarrow H^{+} + OH^{-}$$

At the cathode, hydrogen ions accept electrons and become atoms of hydrogen.

$$2H^{+} + 2e \rightarrow 2H$$

Since the electrolyte must remain electrically neutral, the positively charged ferrous ions (Fe^{++}) often are oxidized to ferric ions (Fe^{+++}) which react with the negatively-charged hydroxyl ions to form ferric hydroxide, or rust.

$$Fe^{++} + H_2O \rightarrow Fe^{+++} + 3OH^{-} \rightarrow Fe(OH)_3 \quad \text{(rust)} + H$$

If enough hydrogen accumulates at the cathode, it becomes polarized; i.e., a very thin film of hydrogen will cover the metal surface which prevents the direct contact between the migrated electrons and the cathode. Therefore, a very thin hydrogen membrane will be constructed and behaves

as a non-porous coating surface to cut off the direct contact of the corrosive ions and the metal. Consequently, the corrosion attack is minimized or may eventually cease entirely.

For corrosion to occur at a significant rate, some means of cathodic depolarization must be active. In other words, in the absence of the cathodic depolarization agents such as oxygen or thermally degraded components, the system soon results in a drastic reduction of the corrosion rate. Thus, no serious damage to the metal part occurs. If the corrosion rate continues and more metal loss is evident, an effective cathodic depolarizing mechanism is present. This explains the corrosion mechanism as one of the following schemes. First, the hydrogen atoms combine together to form a molecule and evolve as gas; or they move in the medium as active atoms and attack to the metal, causing hydrogen embrittlement. Second, depending on the oxygen abundance, a molecule of water is formed and leaves the cathode surface, i.e., the ionic membrane is in a weak or permeable condition and is available for corrosion attack.

3.2 Chemical Theory

The chemical corrosion mechanism is one of the corrosion processes which depends on the nature of the surrounding media with which the metal reacts. Corrosion at high temperature in the vapor and/or gaseous phase and corrosion in liquids (non-electrolytes) are classified as chemical corrosion. The following are examples of chemical corrosion.

(a) Gaseous Corrosion - attach by gases and/or vapors when the moisture cannot condense on the metal surface, usually at high temperatures (e.g., corrosion of furnace structures, some parts of internal combustion engines, steam and gas turbine blades, oxidation of metals on heating, etc.). At relatively low temperatures (200-300°F) a visible oxide film begins to form on iron surfaces. The rate of gaseous corrosion is affected considerably by the composition of the corroding medium.

(b) Corrosion in non-electrolytes - attack in liquids which are non-conductors of electric current (e.g., in various organic liquids, in alcohol, benzene, etc.).

Electrochemical corrosion can be classified as follows:

(a) Atmospheric corrosion - corrosion in moist gas, e.g., in air, new drill pipes and casing stacks around the rig.

(b) Soil corrosion - attack in the soil (e.g., underground pipe corrosion).

(c) Corrosion in electrolytic solutions, i.e., in liquids conducting electric current (e.g., corrosion of drilling fluids, in sea water, in acid and alkaline solutions).

(d) Corrosion in molten salts.

The above examples represent the most common types of corrosion; however, there are no sharp distinctions between them. Combined corrosion which is due to both chemical and electrochemical processes may occur very often. Corrosion may occur alternately in the electrolyte (drilling fluid)

downhole during the drilling operations and in the atmosphere while changing the drill bit and during fishing operations (e.g., alternate wetting and drying of drilling tools).

As a result of corrosion processes, either chemical or electrochemical, the surface or external appearance of the specimen deteriorates. The extent of the deterioration depends on the environmental factors, i.e., chemical composition of the medium, time of exposure, temperature, etc. The surface becomes dull, dark, rough or pitted and covered with various chemical compounds (corrosion products). Although the mechanism of corrosion may vary with the condition encountered, in all cases corrosion can be classified according to the nature of failure. The general forms of corrosion may be described by:

(a) Uniform or general corrosion which is evenly distributed on the coupon surface. This type of attack reflects the chemical homogeneity of the bulk medium and the intensity of the corrosive agents' attack.

(b) Local corrosion is attack concentrated on individual portions of the surface (corroded spots).

(c) Pitting corrosion is attack concentrated on a very small area.

(d) Intercrystalline corrosion is attack concentrated on the grain boundaries. In intercrystalline corrosion, the change in weight before and after the test is small whereas the decrease in mechanical properties and electrical conductivity is considerable; hence the change of these

properties of the metal is a function of the rate of corrosion.

3.3 Effect of Salts on Steel Corrosion

Evans[20] studied the effect of salts that take part in the actual corrosion reaction at either the anode or the cathode and concluded that the velocity of attack depends largely on whether anodic and cathodic products are soluble or insoluble. The action of salts may be classified as follows:

1. Salts like potassium chloride, potassium sulfate, and potassium nitrate yield a soluble anodic product (ferrous chloride, sulfate, or nitrate) and a soluble cathode product (potassium hydroxide), which increases the velocity of corrosion.

2. Salts like zinc sulfate ($ZnSO_4$) yield a soluble anodic product but an insoluble cathodic product [zinc hydroxide, $ZN(HO)_3$], which shields the cathodic area from diffusing oxygen, slightly diminishing the rate of corrosion.

3. Salts like sodium carbonate (Na_2CO_3), sodium phosphate and potassium ferricyanide yield a soluble cathodic product and an insoluble anodic product, which forms a closely adherent protective skin, usually invisible, over the metal. In such cases, corrosion is almost eliminated. But occasionally at certain points, especially at the aerated spots in the bulk, the film fails to adhere; and at such points, marked localized anodic corrosion occurs. The breakdown occurs quite quickly in more dilute solutions of sodium carbonate.

4. Potassium chromate causes passivity even in those parts to which oxygen cannot diffuse, no differential aeration currents are set up, and there is practically no corrosion. If, however, chlorides are also present in large quantities, the protective film breaks down at the edge; and serious localized corrosion will result. Nitrates act more slowly than chlorides in causing the breakdown of the film but are nevertheless effective.

5. Sodium chloride concentrations will increase the corrosion rate of the iron in air-saturated water at room temperature as shown in Fig. 3. The corrosion rate first increases with salt concentration, then decreases, the value falling below that for distilled water when saturation is reached (26% NaCl). The reason the rate first increases, reaching a maximum at about 3% NaCl (sea water concentration), and then decreases is because the solubility of oxygen in water decreases continuously with increasing sodium chloride concentration. On the other hand, the initial increase appears to be related to a change in the protective nature of the diffusion barrier rust film that forms on corroding iron. In the same way, the alkali metal salts (e.g., DCl, LiCl, Na_2SO_4, KI, NaBr, etc.) affect the corrosion rate of iron and steel.

The corrosion phenomenon has been investigated by different investigators, especially in high-salinity geothermal brines. The high corrosiveness of the environment arises from the combination of the elevated temperatures

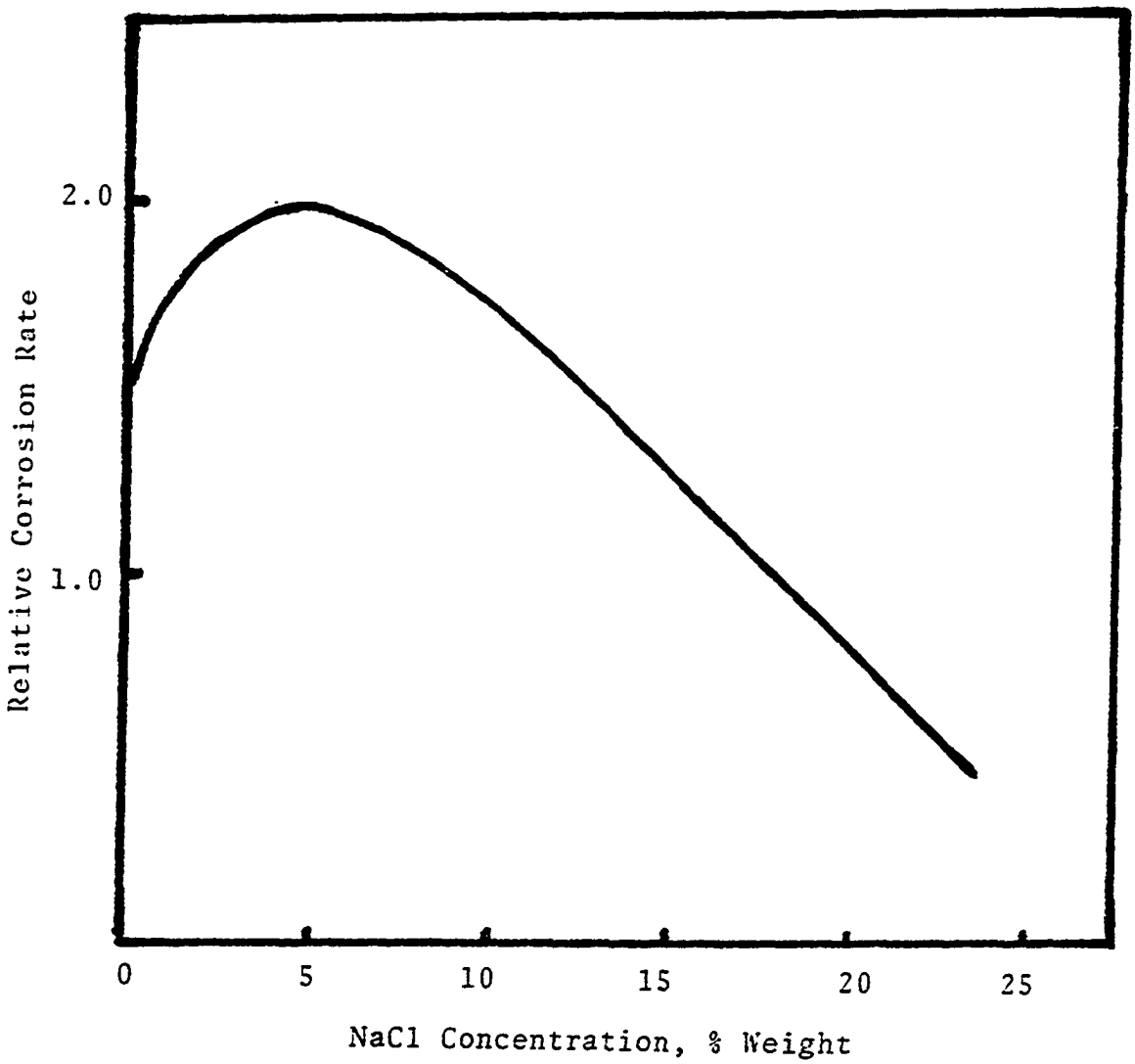


Figure 3. Effect of NaCl Concentration on Corrosion of Iron in Aereated Solution at Room Temperature

(e.g., up to 350°C) and the presence of a high concentration of chloride ions (typically up to 4 M). One should never forget also that hydrogen sulfide is frequently present, although usually only in the parts-per-million concentration range. Nevertheless, sulfide attack might be expected on many of the materials of technical interest used in drilling or well completion operations. Furthermore, the related sulfide-induced failure mechanisms may also impose severe limits on the use of high strength and more expensive alloys in geothermal drilling systems as has been the case in the sour natural gas industry. Accordingly, a major factor in the economic exploitation of geothermal resources will be the cost-effective selection of materials that have sufficient resistance to corrosion to maintain component integrity or using inhibitors to reduce the hydrogen sulfide concentration to a minimum.

3.4 Factors Controlling Corrosion in Drilling Operations

3.4.1 Acid Gases

Acid-forming gases, hydrogen sulfide, and carbon dioxide are the most serious environmental corrosion accelerators that must be dealt with in the drilling fluids. These are often associated with the hydrocarbons of the produced crude oil or gas as well as in formation water and are a major cause of corrosion in the oil industry

starting from the drilling to the refinery processes. Both attack and stress corrosion are caused by them; and they produce highly insoluble corrosion products that often are detected in pits and fatigue cracks of drilling and production equipment, clearly indicating the strong role of hydrogen sulfide (H_2S) and carbon dioxide (CO_2) in the corrosion process.

Contamination of the drilling fluids or produced fluids by carbon dioxide or hydrogen sulfide from the formation can be quite serious if a large amount of gases are introduced from the formation to the fluid column. This is best minimized by properly controlling the hydrostatic pressure. When the drilling operations are at a pressure near that of the formation or at underpressure, larger quantities of formation gases can enter the mud and more acid contamination will occur.

So, it is customary to provide a continuous alkaline buffer to help neutralize them. Usually, the alkaline buffer is used to preserve drilling fluid properties as well as to reduce corrosion problems. Caustic soda, as an alkaline medium, has limitations and may be insufficient to neutralize the acid gases if serious contamination is occurring. However, an arrangement should be considered to facilitate the escape of the gas or for adding gas scavengers to reduce the amount to a minimum.

Primary control against the presence of hydrogen sulfide (H_2S) is necessary because it is very toxic, especially for the safety of the rig crews. Metallic salts can be added to the fluid to precipitate the sulfides and reduce the danger. These materials, such as zinc oxide or zinc carbonate, are used to combine with sulfide ions to form highly insoluble precipitates in strongly basic muds. This reaction reduces the harmful effects of the sulfides from a health standpoint and possibly aids in mitigating corrosion. However, the long-term effects of a continuous buildup of a zinc sulfide precipitate in the drilling fluid is unknown and may become a problem, especially in high temperature geothermals. Also, if pH is lowered due to that chemical reaction, hydrogen sulfide can be regenerated.

Acid gas contamination has resulted from drilling fluid materials that have been altered by temperature,[12,20] microbiological activity,[15] or electrochemical effects.[19] Serious breakdown of many commonly used organic materials containing carbonyl or sulfur-oxygen groups in carbon dioxide or hydrogen sulfide begins at approximately 150°C (300°F). At this point, thermally stable materials should be used when well temperatures are expected to exceed the 300°F range for extended periods of times because thermal degradation tends to destroy drilling fluid properties.

3.4.2 Velocity

There are two major factors to consider in arriving at a design velocity in a particular system which yields

minimum corrosion rates for the drilling equipment (mild steel 1018).

First, the fluid velocity must be high enough to keep the majority of any solids entrained in the drilling fluid and prevent excessive deposition in the circulation system. In practice, the annular velocity, which is the rate at which the fluid rises in the annulus, ranges between 100 to 200 ft/min and 125 ft/min optimum. The obvious consequences of solids deposition are the creation of sites for concentration cells and bacterial growth beneath the deposits. Even if solid deposition is minimal, bacterial activity is always more likely in low-velocity areas such as tanks, pits, and filters.

Second, the velocity must not be too high because if the mud contains solids, erosion, corrosion or impingment may result, especially at connections and elbows. Partially protective corrosion-product films may be stripped off, resulting in increased corrosion rates. This is a particularly severe problem in sweet environments because of the fragile nature of iron carbonate.

The primary difficulty in selecting a design velocity for a particular system is the many purposes desired to be fulfilled by such carrying capacity--corrosion-erosion, maintaining the liquidity of the mud, lubrication of the drill bit, etc. Experience and research indicates that the lower velocity is approximately 1.6 ft/sec and the higher is about

3.2 ft/sec. The optimum annular mud velocity is 2 ft/sec, which would be a safe value.

The velocity in the test was not constant because the velocity of the flow is indirectly a measure of the pressure drop across the inlet and outlet (Δp) which the system failed to keep constant. The reason was that there was no pressure relief valve at the inlet and no pressure regulator with a by-pass line with a two-way valve to maintain a constant pressure drop between the two points. With these, the flow velocity may be stabilized.

3.3 Methods of Preventing Corrosion

The methods used to prevent corrosion are many and diverse. They can be classified as follows:

I. Methods based on modification of procedure
   - (a) By attention to design of structure
   - (b) By attention to surface conditions
   - (c) By application of cathodic protection

II. Methods based on modification of environment
   - (a) By de-aeration of water or aqueous solution
   - (b) By purification or dehumidification of air
   - (c) By addition of corrosion inhibitors either organic or inorganic

III. Methods based on modification of metal
   - (a) By increased purity
   - (b) By addition of alloying elements
   - (c) By heat treatment

IV. Methods based on protective coatings

(a) Coatings of reaction product (chemical or electrochemical treatment of metal surface)

(b) Organic coatings: paints, resings, etc.

(c) Inorganic coatings: enamels, cements

(d) Temporary protectives

(e) Metal coating processes, as follows:

1. Coatings produced by "cladding": Rolled-on coatings such as pure aluminum on aluminum alloys
2. Coatings produced by "hot-dipping": Galvanized iron, tin plate
3. Coatings produced by metal spraying: zinc and aluminum are the most common
4. Coatings produced by "cementation": sherardizing (zinc), calorizing (aluminum)
5. Coatings produced by electrode deposition: A wide range, including Cd, Ni, Cr, Ag, Rh, and co-deposited coatings.

With a close look to the above corrosion prevention techniques, it is possible to indicate that, first, a given method of prevention is not necessarily applicable to all metals in the same environment. Secondly, the methods listed must not be regarded as necessarily mutually exclusive. Moreover, the choice between one method and another must be determined by economic and other factors under the actual conditions of service.

3.6 The Economic Potential of Corrosion and Corrosion Research

It is by now a well-known fact that corrosion causes costs of considerable magnitude for modern industrial societies. For instance, the National Bureau of Standards and the Battelle Columbus Laboratories estimate that the total annual cost of corrosion to the United States is about $70 billion, or 4% of the Gross National Product, and that $10 billion of this total cost, or about 0.6% of the GNP, could be avoided by the use of presently-available corrosion control technology.

Passaglia[4] gave two sensible questions that should be asked in an attempt to declare the importance of corrosion research. The first is "What would the Gross National Product be without the developments in corrosion control technology of the past sixty years?" The second question, which is harder, is "Why is the cost of corrosion a constant at 3 to 4% of the GNP?" To answer the first question, it is necessary to see what technological advances would have been impossible without advances and development in corrosion monitoring, morphology and control. The outputs of corrosion control technology development may be classified into the following types: (1) metallurgical improvements of the material, (2) new and effective techniques of corrosion control to motivate new technological advances and machine construction, and (3) new and efficient methods of design.

To manipulate and study the effect of all of these on the advances and development of the technical industry needs a significant research effort.

CHAPTER IV

EXPERIMENTAL DESIGN

Under the recent great demand of deep drilling in the search for oil, the downhole equipment is usually under very severe conditions of temperature and pressure, acid gases and salt contamination, thermal degradation of the fluids, etc. These factors combined together accelerate the chemical reactions between fluids and metal surfaces and also aggrevate the metal corrosion. The test is made by two different techniques. The first technique is a linear flow system using the modified flow loop designed in the Petroleum Engineering Department. The second is a rotation or rolling technique using the Baroid rolling oven. In a successive trial, the two approaches were combined by designing a new cell (Magcorrosion cell) in which the fluid is flowing linearly in the flow loop and rotates around the coupons with variable controlled speeds of rotation. A static technique was also used.

4.1 Flow Loop Corrosion Test

4.1.1 Sandia-Lab Flow Loop

The entire loop contains about 260 ft of 1/4 inch O.D. and 0.035 inch thick stainless steel tubing. The pumping,

measuring and recording system are discussed in detail in reference 21.

4.1.2 PGE Flow Loop

The closed system mud flow loop (from its design point of view) simulates the actual circulation system of the drilling fluid in the drilling operations in the following aspects.

1. The pumping system consists of a speed-controlled-motorized feed pump passing the mud to the big single-positive-acting pump to circulate mud from the reservoir under surface conditions to the hot section, passing through the cooling system back to the reservoir. The hot section is thermally controlled by temperature controllers and indicators along with iron-constantan thermocouple sensors located at different spots in the loop, all of which are connected to a twelve-channel temperature recorder. The test temperature can be adjusted to the required temperature which corresponds to a certain depth by a heating element wired with an electric built-in relay controller system to admit the required amperage to heat up the heater to the desired temperature. The heating element is stuck to the 3/8" O.D. stainless steel seamless tubing and cemented inside a 4 inch O.D., 1-1/2 inch I.D. fiberglass asbestos insulating tube to minimize the heat loss. The rest of the lines are well insulated with a fiberglass blanket all the way to the hot end (Magcorrosion cell).

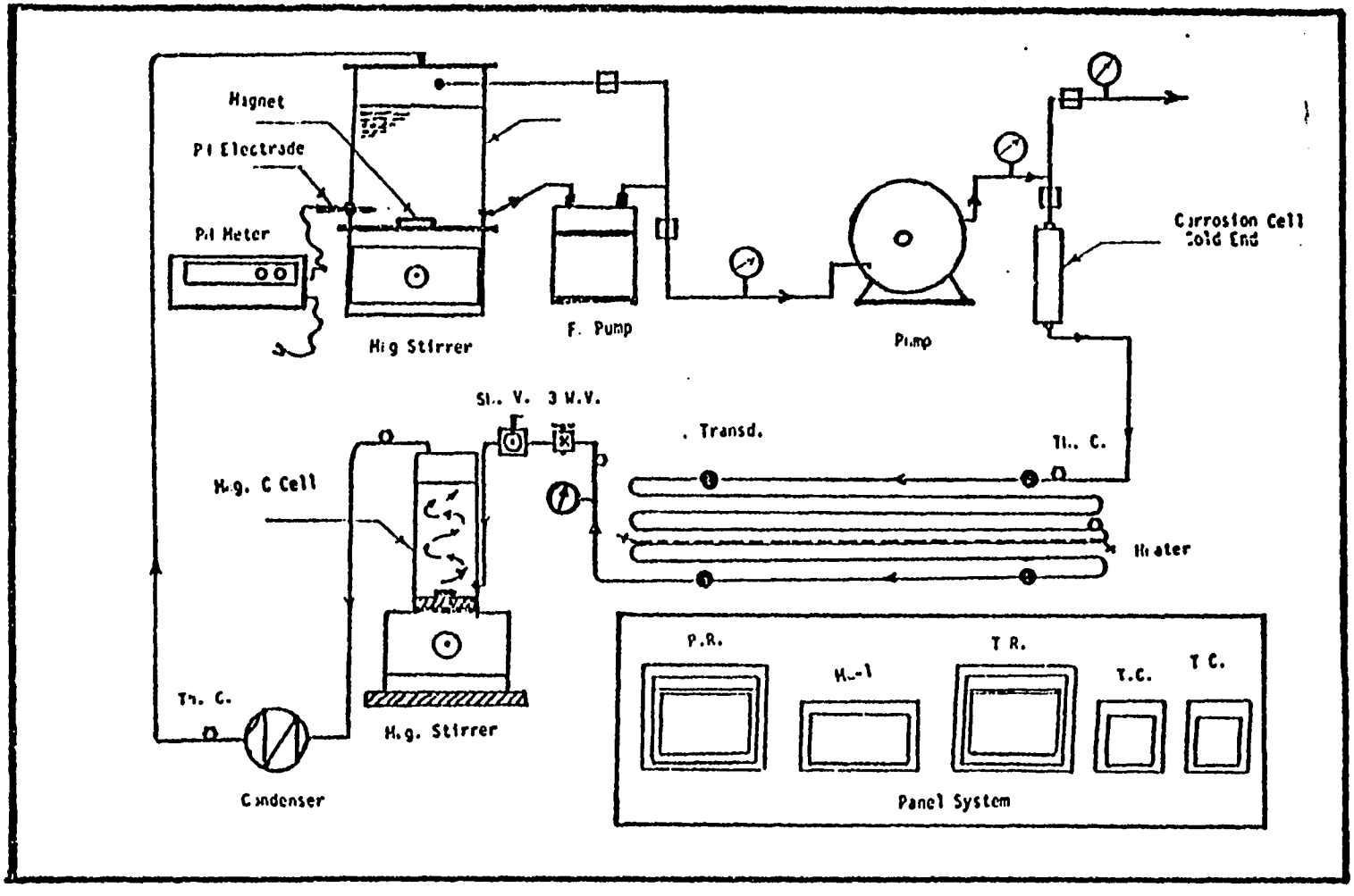


Figure 4. Schematic Diagram of the Dynamic Corrosion Test - PGE Flow Loop (Closed System)

2. The shearing system simulates the nozzle shearing due to the hydrostatic head of mud. The Magcobar nozzle shear valve, Fig. (5), was hooked up in series with the loop immediately after the Magcorrosion cell. The purposes of this valve are: (1) to shear the drilling fluid and (2) to be used as a back-pressure regulator to maintain adequate pressure differential in the system with appropriate scale, corresponding to the differential pressure between the formation pressure and the hydrostatic head of the mud column.

3. The pressure system: The pressure in the system is well controlled by a pressure transducer system, Model DP-15-3000 psi absolute inlet and outlet and ± 50 psi differential, connected with the Validyne MC1-10 channel pressure digital indicator which is also connected to a twelve-channel double scale, ten-inch strip chart recorder. The hydraulic system diagram is shown in Fig. (6a, 6b, and 6c).

4. The corrosion cells: There are two corrosion cells. The one fixed at the cold end shown in Fig. (25) is 1 inch O.D. nine inch-long stainless steel tubing. It can be opened at both ends with 1-inch swage-lock fittings in order to insert the coupon carrier. The other cell, fixed at the hot end. Magcorrosion cell, Figure (7), is 316-stainless steel heavy duty cell. It has inlet and outlet ports plus a two-way ball valve. The coupon holder is installed in the stainless steel housing at the bottom of the cap. The specimens are completely isolated from the metal to eliminate the flow of the electrolytic current between the coupons and the cell

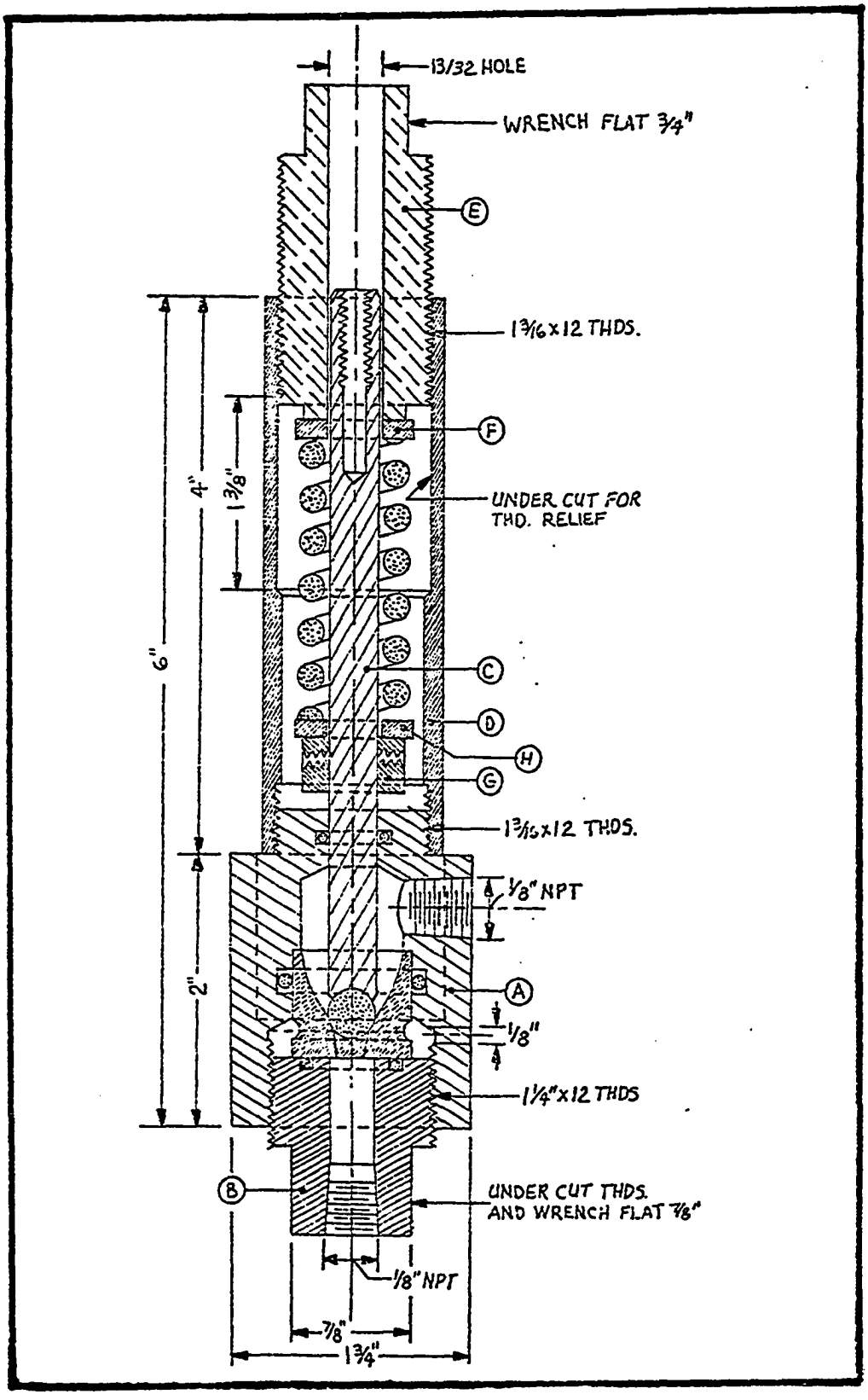


Figure 5. Shear Valve

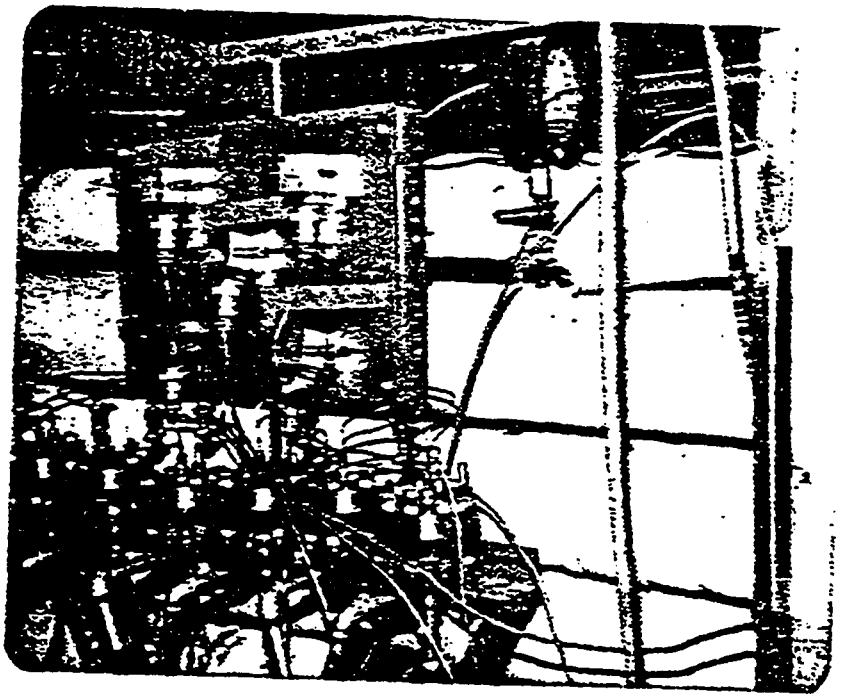


FIGURE 6a: The hydraulic system of the transducers.

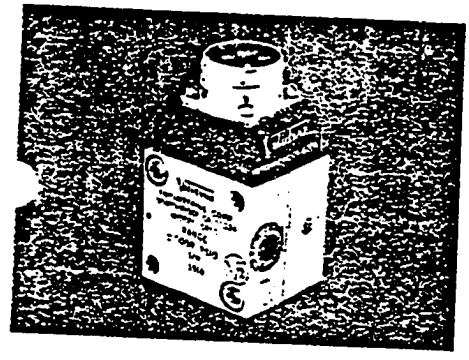


FIGURE 6b: Pressure transducer DP-15 assembly.

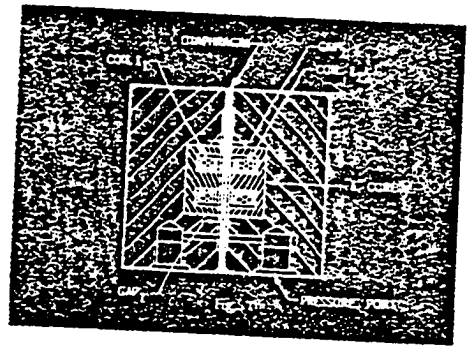


FIGURE 6c: Pressure transducer DP-15 cross section

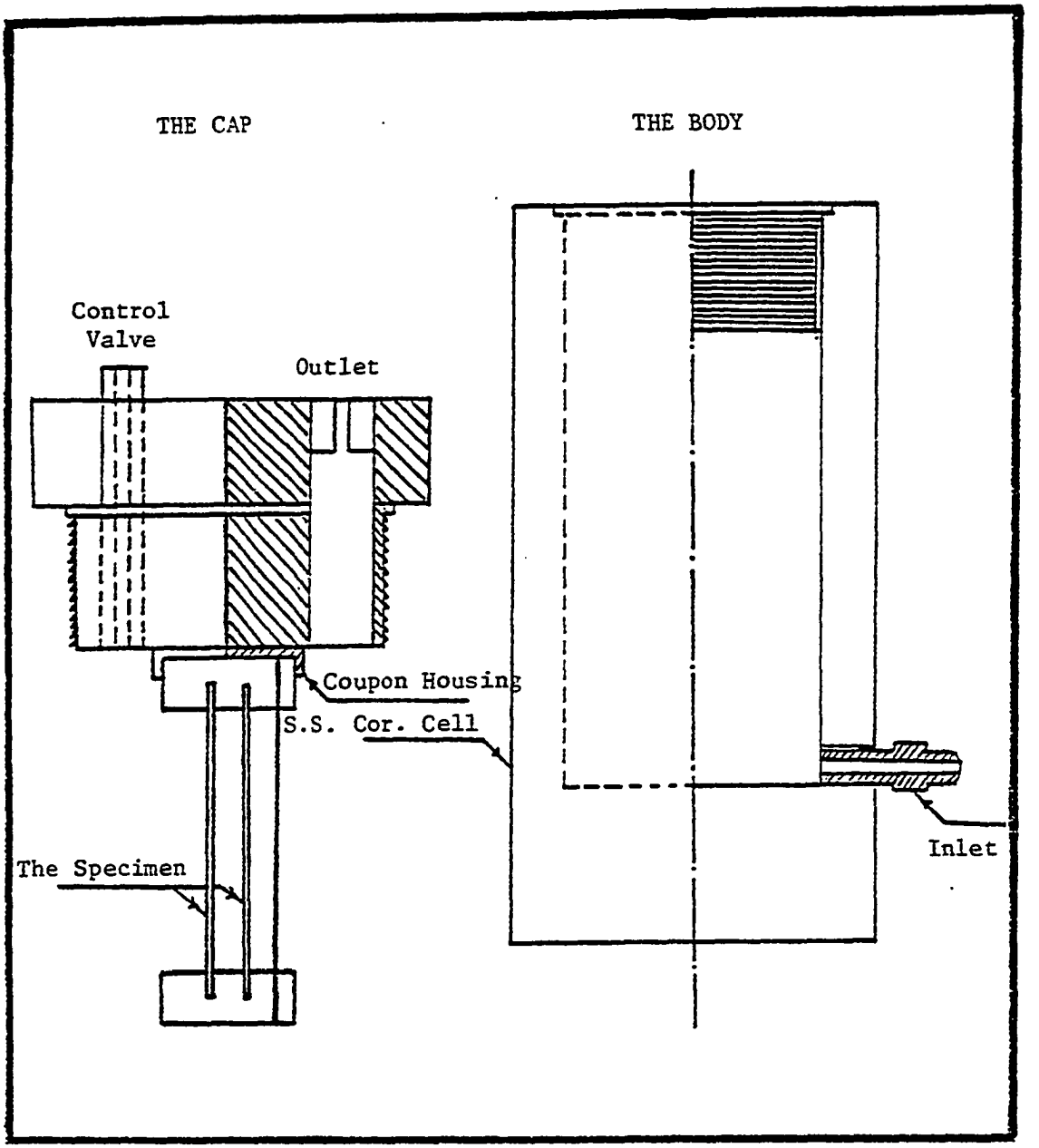


Figure 7: Mag-Corrosion Cell

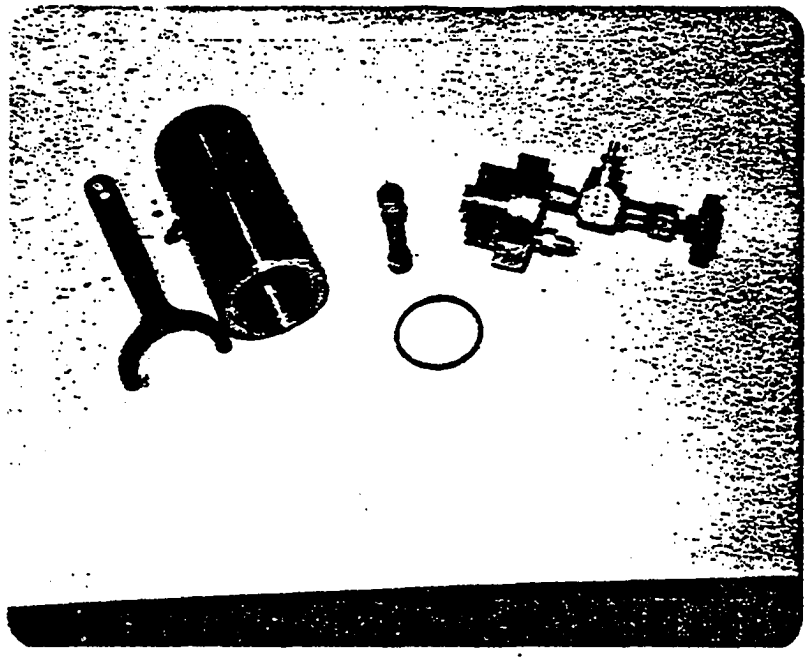


Figure 8: Mag-Corrosion cell parts.

body which may affect the corrosion measurements. The cell was seated on a magnetic stirrer to rotate the fluid in the cell with controlled speed, simulating the fluid rotation under the effect of the drill bit rotation and bottomhole conditions.

4. pH, which is a measurement of the hydrogen concentration in the solution, is instantaneously monitored using a digital pH meter during the run by a pH probe immersed in the reservoir. The pH value is maintained at the desired value by adding caustic soda as necessary. The pH of the drilling fluid represents the main variable which needs control in order to avoid undesirable failure of equipment.

The small mud flow loop is designed to try to eliminate the line-plugging problems, especially in higher-temperature runs, due to the gelation of the common drilling fluid components such as bentonite. All flow lines are either 1/4 inch or 3/8 inch and connections are made of seamless stainless steel which is non-corrosive with the bulk at the test conditions. The number of connections (fittings) in the flow lines has been kept to a minimum to reduce pressure loss and line plugging. The flow velocity has been determined to avoid the solid sedimentation, especially in the vapor phase in the hot section.

Two-ball system check valves are installed at both the inlet and outlet of the Wallace positive-single acting pump in order to pump the drilling fluid properly to the system.

6. The Reservoir is designed to eliminate any air contamination during the test. Inlet and outlet ports and a bypass line to maintain the pumping capacity of the feed pump coincident with the suction capacity of the big pump. The pH probe can be inserted in the reservoir through a 1/2 inch hole with a rubber stopper. It has a cover to close tightly with four long screws if necessary. The reservoir is seated on a strong mag stirrer to agitate the fluid externally without air intrusion to the system.

4.1.3 Correlation Between the Two Loops

The small and simplified PGE flow loop was fabricated as a part of a steamochemical project at the School of Petroleum and Geological Engineering. The loop can handle the stabilization and corrosion tests of the drilling fluids efficiently. Some changes have been made to overcome some problems experienced with the Sandia-Lab flow loop. These changes were: (1) Due to the high gelation tendency of most conventional and geothermal muds at high temperature, the possibility of line plugging was too high. Therefore, the flow lines in the hot section of the small loop were made of 3/8 inch O.D., 0.25" O.D. seamless stainless steel tubing and the number of constrictions and fittings were kept to a minimum per line. (2) Since the system is under temperature, pressure and shearing control, and the mud should experience the change of temperature from the surface to bottomhole to surface again during each circulation, the scaling rule for the loop and the time of exposure of the drilling fluid at

any reference depth does not require a very long heating section. For this reason, the PGE loop has only one heating section, is perfectly insulated and wired with temperature controllers and recorders to monitor the temperature. This way, the risk of plugging is minimized and maintenance and operating expenses are less. (3) From the corrosion-monitoring point of view using the weight loss technique, the PGE loop can be used efficiently like the Sandia-Lab one. However, in this study a new Mag-corrosion cell was fabricated to study the effect of the combination of the two fluid motions in the vicinity of the drill bit downhole, i.e., rotation due to the drill bit and vertical motion from the bottom up to the surface, on the corrosion phenomena. (4) Three-way shunt valves have been used in the small loop to obtain additional control and avoid the deflection of the transducer diaphragm when exposing it to the pressure head from one side and atmospheric pressure from the other while calibrating or flushing the system.

4.2 Rolling Technique

The corrosion rate was measured by the weight loss technique under the rolling condition and elevated temperatures. The different types of drilling fluids are formulated in the laboratory using various components and percentages to obtain the desirable characteristics for performing well under such conditions.

The Baroid rolling oven, as shown in Fig. (9), is thermally controlled and the temperature varies from 0-550°F. The oven has only one rolling speed with indicating lights. The main purpose of the mud rolling is to keep the fluid in a moving condition while raising the temperature to obtain accurate measurements of the mud characteristics at the desired test condition. Two stainless steel cells were designed to hold the coupon holder rigidly, as shown in Fig. (10). Also there is no metal connection between the coupons and any metal surface during the run.

The test was done at four different temperatures (200, 300, 400, 500°F) for each drilling fluid with rolling. The corrosion rate measured under these conditions is more accurate because (1) the fluid in the hole is moving--not stationary; (2) the fluid under rolling is continuously agitated without settlement, simulating the fluid motion across any specific depth.

4.3 Static Technique

The static technique is used to measure the fluid corrosivity under a stationary condition (no circulation of the drilling fluid) which occurs for a period of time very often in the drilling operation. This usually happens when (1) changing the drill bit; (2) differential sticking of the drill pipe occurs; (3) running casing; or (4) fishing broken or missing tools at the bottom of the hole. Thus, the cells used in the rolling test were used to measure the corrosivity

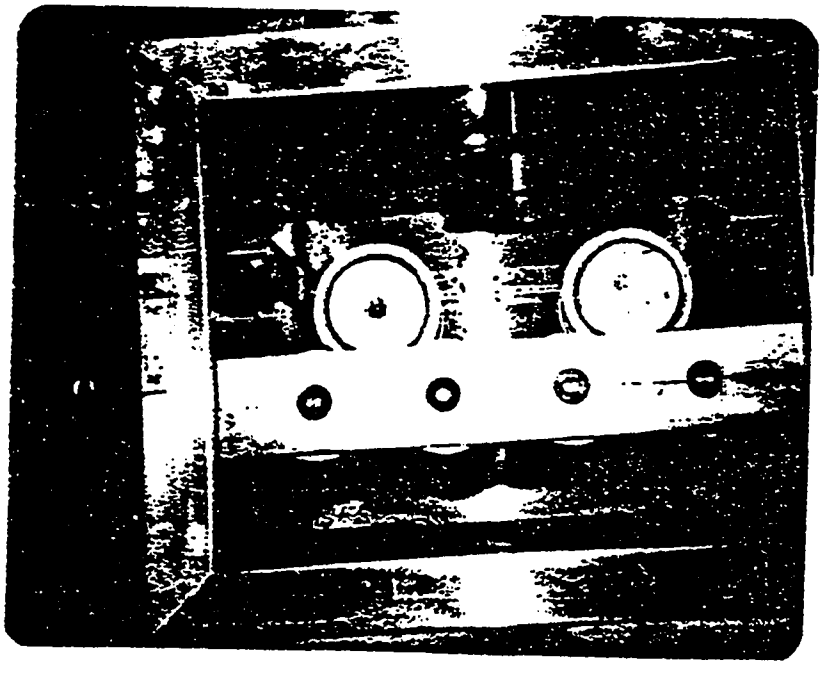


Figure 9. Baroid Rolling Oven With the Cells

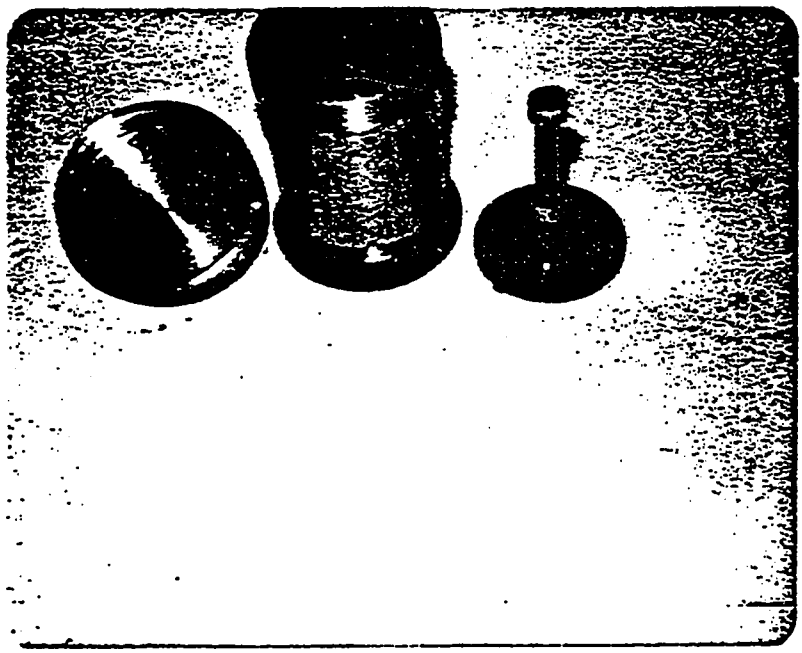


Figure 10. Rolling Technique Corrosion Cell

of the fluid under static conditions by loading the coupon holder with the test specimens and inserting it in the fluid. The cap was screwed on and left for a period of time. The tests were run at elevated temperatures (200, 300, 400, and 500°F). Correlation and analysis between the results obtained from the loop, rolling and static tests were made.

4.4 Pressure Transducer Calibration

4.4.1 Equipment Zero Process

4.4.1.1 Pressure Transducer (DP-15-3000 psia) absolute

1. Put the 3-way (shunt) valve in drain position (the position in which the capillary is in the atmosphere) for the inlet line of the system.

2. Set arbitrary zero on the corresponding channel on the MC-1-10 Demodulator.

3. Attach the master gauge (calibrated with dead weight tester) in series with the hydraulic load cell. Also attach a suitable tubing connection with the positive and negative sides of the DP-15-3000 psi transducer.

4. To make sure that the transducer does not contain any air bubbles on either side of the diaphragm, loosen the two allen screws on both sides of it until you receive liquid, then tighten it carefully.

5. Steadily load the transducer statically with the hydraulic cell up to 3000 psi on both sides of the diaphragm and observe the zero reading. Adjust if it is required.

4.4.1.2 Pressure Differential Transducers (DP-15 ± 50)

Case 1. Pressure above 1.0 psi D.

Use the same procedure above except apply no more than +50 psi to avoid diaphragm deflection.

Case 2. Pressure less than 1.0 psi D.

Use a water manometer attached to the positive and negative sides of the transducer with a plastic tube through the 3-way shunt valve, drain, transducer and the manometer. Every one foot of water will balance 0.433 psi hydrostatic head so every one inch of water head will balance 0.03608 psi, which is accurate enough.

4.4.2 Equipment Readings

After zero is set, the tubing connection is changed by one line to one side, either the positive or the negative side. However, attaching to the positive side will give positive readings and attaching to the negative side will give negative readings. Either is acceptable for the purpose of calibration.

6.2.1 Pressure Differential Transducers

1. Inject fluid (mineral oil) to pressures of 10, 20, 30, 40 and 50 psi, and set the span for the channel used on the MC-1 demodulator.

2. Release the pressure with the hydraulic pump from 50 down to zero in 10 psi increments. Watch the readings and zero.

3. If zero is not obtained, set to zero and repeat steps 1, 2, 3, and 4 until zero is reached.

4. Loading the transducer with pressure statically to simulate the test conditions may be required.

6.2.2 Absolute Pressure Transducers (0-3000 psi) Diaphragm

1. Inject fluid (pure mineral oil) at 1000, 2000, 3000 psi and set span for each stage.

2. Reduce pressure down to zero in 1000 psi increments to check the readings. Adjustments and rezeroing may be required if the zero reading is not obtained.

CHAPTER V

TEST PROCEDURE

5.1 Mud Preparation

Different formulations of fresh-water-base mud were prepared in the lab. These fluids consisted of bentonite clay, sepiolite clay and resinex in various amounts. Variable amounts of caustic soda and sea salt were added. These mud batches were mixed in the Magcobar multimixer for a long enough period to age the drilling fluid and evenly distribute the clay particles and chemicals throughout the liquid phase.

The mixing process, however, may also be accomplished by the flow loop. The solids must be divided into portions of about 30-35 grams. The portions are added periodically every two or three complete circulation cycles while the mag-mix is working under the reservoir to keep the fluid in a stirring condition. The hydration period is primarily for liquid-solid adsorption or chemical dispersion. Naturally, clays are sensitive to water contact and disperse proportionately with time.

The test herein actually has a dual purpose. The first is to formulate a mud of commercially available

material, chemically and thermally stable with time of exposure under bottomhole conditions. The second is to minimize its corrosivity under these prevailing conditions.

5.2 Corrosion Test (Flow Loop)

The specimens (coupons) were cleaned (according to NACE and ASTM standards) and weighed. The corrosion cells (cold and hot) were loaded with the coupons and installed in their places in the flow loop. Water circulation was initiated for 30 minutes to make certain that the pumps and transducers were working properly. Di-methyl blue was injected followed by the agitated drilling fluid to drain out all the water in the lines. The fluid was then circulated at room temperature for about 40-60 minutes. Before increasing the temperature of the system, the pressure drop in all test section flow lines was recorded, and the apparent viscosity was calculated. At the same time, a fluid sample was taken and the rheological properties were measured(ϕ_{600}, ϕ_{300}, PV, YP, IG, and 10 minutes' gel) using a Baroid variable speed rheometer at room temperature. Consistency between the two values of the viscosity was required before the test was initiated at an elevated temperature. The test temperature was raised gradually from room temperature to 200, 300, 400 and 480°F maximum. In some runs the temperature was raised in 50°F increments instead.

5.3 Test Duration

The flow loop corrosion test was conducted for a period of time long enough to allow a reliable measurement of the steady state corrosion rate by weight loss techniques. The time required depends on:

a. The test materials

b. The corrosivity of the bulk fluid (mud)

c. The equipment efficiency (pumps, transducers, heating elements, thermocouples, etc.)

As the duration of the test increases, more stable corrosion rates will be obtained, and the weight loss technique is more effectively used.

The transducers' absolute and differential data were recorded every 15 minutes in some runs and every 5 minutes in others. The reason for this was to make certain that the fluid was flowing properly. The maximum absolute pressure in the flow loop was 3000 psi. Pumping pressure was adjusted around 1200 psi using the nozzle shear valves. However, maintaining the system pressure was a difficult task because of the pump problems and the temperature thinning or gelation effects which required continuous adjustments to the shear valves. As the system pressure went down, the shear valve tensions were increased. Caution was taken to work with the shear valve at a temperature higher than 300°F. The absolute pressure of the system was maintained higher than the vapor pressure of the circulated fluids because, if the system pressure is less than the vapor pressure at the test temperature,

the fluid will be transferred to the vapor phase. In this event, (1) the fluid flow is not laminar but turbulent; (2) solids may be precipitated by gravity onto the tube wall causing plugging of the lines; (3) handling the shear valves is more dangerous; (4) the reliability of the test is reduced; and (5) fluid vapor may leak to the capillaries to the transducers which may affect the diaphragm's accuracy.

5.4 Pump Maintenance

The Wallace triplex metering pump limited the testing period considerably. The drilling consistency reduced the pump efficiency. The slurries tested, at varying times, scoured the plungers and packing such that continuous leakage occurred. The spring seated ball check valve used also gave much trouble due to the adherence of dirt and solids around the spring which immediately reduced the efficiency of the valve operation. This can be observed when the system pressure is reduced to zero or vibrates by 200-300 psi. Once one check valve of the total six became inoperative, the flow rate would be reduced. The packing material was changed to a harder material so that it could stay working longer with all types of drilling fluids. Also, the check valves were replaced by two ball valves which proved more efficient with our system.

5.5 Test Specimen

In general, the size and shape of a specimen in the corrosion test may vary with the purpose of the test, the nature of the materials to be tested, and the testing apparatus to be used. The size may also be limited by the necessity of preserving a proper ratio between the area of the specimen and the volume of the testing solution (drilling fluid) when the latter must be limited. Efforts were made to have the ratios of surface to mass large, and the edge area to total area small. The shape and dimensions of the specimen were such as to permit weighing on an accurate balance and to facilitate accurate measurement of dimensions which were made to the nearest 0.01 in (0.25 mm).

All sheared edges were trimmed beyond the shear marks by sawing, machining, filing and/or grinding. The final cuts obtained were very light so as to minimize hardening and distortion of the edges.

There are several standard recommended practices for preparing, cleaning and evaluating corrosion test specimens (ASTM); however, the most practical procedure is the following:

a. Degrease the specimen in an organic solvent or hot alkaline cleaner.

b. Give it a preliminary chemical treatment (pickling) in an appropriate solution or surface the specimen with coarse abrasive paper or cloth, such as No. 50.

c. Resurfacing with No. 120 abrasive paper or cloth or the equivalent is required to obtain a smooth clean surface.

5.6 Number of Specimens

Two coupons were used in the corrosion cell in every run for either the flow loop or rolling technique. However, the corrosion cell is mainly designed for four coupons plus some 1/16" diameter rods. The main reason for using only two coupons in all our tests was to maintain a proper ratio of the surface area of the coupons to the volume of the drilling fluid and also to obtain a measurable corrosion effect on each coupon immersed in the fluid.

5.7 The Sample Preparation

In the test to measure the corrosion rate or to evaluate an inhibiter, the coupon surface preparation was accomplished by surfacing it with a coarse abrasive paper (No. 50) to remove the surface layer of the specimen. However, in order to simulate actual field applications, the coupons should not be highly treated chemically or mechanically either before or after the test. The final treatment was to surface with No. 120 abrasive paper and then degrease it with acetone or just by washing under running water with solvent. Once cleaned and dried, the specimens were then weighed accurately (within ±0.0005 gr. accuracy). The coupons were

placed carefully in every cell (two coupons each) without any contamination and the run started. The duration of the test was measured to 0.005 hour. The temperature was adjusted to room temperature for one hour for each test, then raised successively to 200°F, 300°F, and 400°F, depending on the capabilities of the system and the mud stability. After exposure, the time, temperature, pressure, pH and the rheological properties were listed and the coupons were cleaned and weighed after the run with the same accuracy. The coupons were cleaned after the test using a rubber scrubber under running water.

CHAPTER VI

ANALYSIS OF TEST RESULTS

The rheological properties of the drilling fluids are considerably sensitive to the temperature of the environment. In the case of deep well operations and geothermals, high temperatures, combined with shear at the bottomhole, might create gelation and flocculation problems. The yield point of the testing fluids used under these severe conditions also varies with temperature, especially after the flocculation point of the fluid. Beyond this point, the yield increased considerably. Therefore, in order to achieve a successful drilling operation, the mud must be thermally stable and noncorrosive.

Sodium hydroxide (caustic soda) was used as a corrosion inhibitor for the following reasons.

1. It is a commercially available and inexpensive type of chemical.

2. It is a strong electrolyte and can be considered as a continuous supply of the hydroxyl group (OH^-) which combines with the hydrogen ion (H^+) to form a water molecule. In other words, it decreases the severity of hydrogen attack on the metal (hydrogen embrittlement).

3. Increasing the pH (alkalinity) of the drilling fluid decreases the corrosion rate as shown in Figure 21 because it neutralizes the acidity of the solution due to the higher solubility of the acid gases with temperature and pressure.

4. It performs well with the rheological characteristics of the drilling fluids.

Rolling techniques using a Baroid Rolling oven and the special corrosion cell shown in Figure 9 were used to measure the corrosion rate at 200°F and 300°F (Tables 1 and 2, respectively). The corrosion rate decreased with increasing pH of the mud. Rolling the fluid and the specimen together simulates the rotation of the drill pipe and the fluid under the bottomhole conditions. The rolling test was extended to high temperatures, beginning from 200°F to 500°F. This technique used in the study can be considered as an open system because oxygen escaped upon sample exposure to the atmosphere. The results in Table 11, which are a summary of the results tabulated in Tables 7, 8, 9 and 10, are plotted separately for each cell as shown in Figures 11 and 12. This indicates that the average corrosion rate in the open system increased with temperature to a certain limit and then declined rapidly due to the escaping of the oxygen at higher temperatures. Also, it is noticed that the volume of the drilling fluid in the temperature range between 400°F and 500°F decreased to about 80% of the original volume. This may be considered also as a reason why the corrosion rate decreased at temperatures higher than 400°F due to the fact

that an insufficient volume of drilling fluid can lead to exhaustion of the corrosive constituents.

The gelation tendency of the drilling fluid at higher temperatures and high shear in the vicinity of the drill bit gives many problems, especially in deep drilling and geothermals. Therefore, thermally-stable drilling fluids to withstand the bottomhole conditions were formulated. These fluids were tested dynamically in the flow loop to evaluate and modify their composition. Sepiolite clay, which is extremely stable at high temperature, was added to improve the bentonite clay mud. Sepiolite combined with bentonite in equal proportions was used along with a third component (resinex) to formulate the thermally stable muds B_2, and B_3. The difference between them was the differing amounts of caustic soda (NaOH) and sea salt additives. The liquidity and gel strength of the test fluid was observed after every run in the rolling oven, and the plastic viscosity was measured using a V.G. Rheometer. The samples to measure flow rate and rheological properties, such as plastic viscosity, yield point, and gel strength, were taken from the loop through a 3-way valve at room temperature. As shown in Table 12, the flow rate was very stable with averages of 0.8864 cm^3/sec at a temperature of 400°F for two hours and 0.9693 cm^3/sec at 450°F for one hour. The fluid in each cycle experienced high temperatures in the hot section and cold temperatures immediately after the heat exchanger section.

The stability also is indicated by the readings of the pressure differential transducers of 1/4", 3/8" and 5/8" capillary viscometer. There were approximately equal readings of the pressure differential which ranged from 0.83 psi at 1200 psi inlet/1100 psi outlet to 0.95 psi at 1350 psi inlet/1250 psi outlet for the 1/4" tube.

Corrosion rates measured for mud B_1 are tabulated in Tables 13, 14, 15 and 16 using the flow loop and rolling techniques. They are plotted in bar diagrams shown in Figures 13, 14 and 15. The test results can be summarized as follows:

1. The corrosion rate at the hot end is much higher than that at the cold end in the flow loop, indicating that the temperature and the dynamical condition of the drilling fluid in the flow lines accelerate the corrosivity of the fluid.

2. The corrosion rate is reduced when the fluid alkalinity is increased (pH raised from 9.81 to 11). However, the hydrogen content decreased with the temperature as shown in Figure (16). Consequently, retaining high pH is required.

3. The corrosion rate is relatively low in the case of distilled water base fresh mud. However, it is higher with tap water due to the presence of the chlorine ion which accelerates corrosion.

4. The corrosion in the case of rolling in which the specimen rotates with the fluid at high temperature is lower than that of the hot end of the flow loop, whereas it is about equal to that of the cold end.

A comparison between the corrosion rates measured by the PGE and Sandia-lab flow loops for the same drilling fluid is shown in Figure 17. The results as tabulated in Tables 17 and 19 indicate that the cold end corrosion rates are almost equal (12.197 mpy - 11.684 mpy, respectively); however, at the hot end, the corrosion rate is higher in the PGE loop (26.136 mpy - 21.778 mpy, respectively). This difference is actually due to the uncontrollable temperature of the hot section in the PGE loop and the attachment of the new mag-corrosion cell on the PGE flow loop. This cell incorporated in the system added the rotational motion to the fluid. However, sometimes the corrosion rate was different from one coupon to another, even in one cell. The corrosion rate is dependent upon the homogeneity of the drilling fluid (i.e., the distribution of the chemical additives in the bulk) and the uniform exposure of the coupons to it. This might reflect the various types of corrosion (for instance, uniform corrosion, spot corrosion) which are eventually dependent on the reliability of the experimental parameters and how far the corrosion-rate effect factors can be manipulated. The test duration in the Sandia-Lab loop was for five hours, 2 hours at 80°F and 3 hours (one hour each) at 200°F, 300°F, and 350°F. PGE loop tests lasted 3.1 hours at an average temperature of 250°F.

Rolling technique results shown in Table 18 are compared with data obtained from the two flow loops, linear and rotational flow. The corrosion rate of the rolling

technique of 14.821 mpy is less than 26.136 mpy and 21.778 mpy for the hot ends of the two loops (PGE and Sandia-Lab, respectively). This result indicates that the rotation and linear flow of the drilling fluid around a stationary specimen is much more severe than that of the rotating fluid and the specimen. In other words, the abrasivity of the fluid is higher in the case of the stationary coupons. The rolling tests is run only at elevated temperature due to the fact that corrosion is much higher at higher temperature.

Rheological properties have been examined for drilling fluid B_1 with the Sandia-Lab flow loop. These properties are:

(1) plastic viscosity in centipoise calculated as follows:

$$\phi_{600} - \phi_{300} = PV \quad cp$$

where ϕ_{600} is the dial reading at 600 rpm

ϕ_{300} is the dial reading at 300 rpm

The sample is taken at room temperature and atmospheric pressure.

(2) gel strength, lb/100 ft^2

(3) yield point (lb/100 ft^2) calculated as follows:

$$\phi_{300} - PV = YP \quad lb/100\ ft^2$$

(4) pressure differentials, ΔP 1/4", ΔP 3/8", ΔP 5/8", and the flow rate which were considered as a measure of the fluid stability at elevated temperature.

The summary of the test is tabulated in Table 23 indicating the effect of temperature on the flow rate and

plastic viscosity. As the temperature of the system increased, the flow rate decreased slowly from 14.7 cm^3/sec at room temperature to 14.1 cm^3/sec at 300°F to 11.8 cm^3/sec at 350°F. Behavior of the fluid flow rate and viscosity is plotted in Figure 19. The test period was 9 1/2 hours at high temperature without plugging the lines.

Corrosion cells were loaded during the test to measure and compare the corrosion results in both the flow loop and rolling techniques. The results, shown in Tables 21 and 22, agree with the smaller corrosion rate in the rolling technique at high temperature.

The corrosion rate is measured using a static technique as shown in Table 23, and the interrelationship between the three techniques is shown in Figure 20. The test temperature was 200°F for 12 hours and 300°F for 12 hours for a total of 24 hours exposure time to the coupons. The rolling test was also run under the same conditions. The static corrosion rate is considerably lower than the rolling and much less than that of the hot end in the flow loop. This indicates clearly the effect of fluid velocity and type of flow on metal corrosion.

Mud formulation B_2 contains the same 3 major components, bentonite, sepiolite and resinex, along with sea salt and caustic soda. The physical characteristics measured with a Baroid Rheometer is shown on page 119. The corrosion test using the rolling technique for this mud was made at elevated temperatures of 200°F, 300°F, 400°F and 500°F

in the rolling oven. The corrosion rate obtained for the fluid was very low which is essentially negligible as shown in Tables 24 through 27. The specimens were very clean after the 200, 300 and 400°F tests with no oxide spots, even though the time of exposure was long enough for corrosion to occur. At 500°F in the rolling test, the corrosion rate was increased up to 5.345 mpy, which is still negligible; but it decreases because the pH of the fluid dropped down to 8.25. A summary of the corrosion and pH results is tabulated on page 122 and plotted in Figure 21 to indicate how pH and corrosion rate change with temperature. The point of intersection of corrosion and pH gives the most efficient pH value (9) to keep the corrosion rate insignificant for temperatures reaching 480°F. This formulation of mud is completely non-corrosive and thermally stable up to 500°F as observed in the laboratory.

It is advantageous to divide B_3 mud tests into three groups. All of them have the same fundamental components and the same percentage of each, bentonite, sepiolite and resinex. Different amounts of sea salt and caustic soda were used. Group No. I: The mud contains 1% by weight sea salt and the same percentage of caustic soda. The corrosion test (rolling) results and pH values are summarized on page 128. It shows that the corrosion rate increases moderately with temperature from 2.048 mpy at 200°F and 11.11 pH to 9.621 mpy and 11.12 pH at 400°F. However, at 500°F, the pH dropped considerably to 9.05, and the corrosion rate

increased to 19.199 mpy. This data is plotted in Figure 22 and the point of intersection gives the critical value of pH equal to 9.3 and corrosion rate at 19 mpy, which is considerable with industry.

The mud of Group II contains 10% by weight sea salt and no caustic soda. The pH value was 7.43 and plastic viscosity was 8 cp. Flow loop stabilization and corrosion tests were made, and the results are tabulated in Tables 32 and 33. The rheological properties also are tabulated in Table 34, which gives very stable viscosity values (4.5, 5, 5 cp) at 200°, 300° and 400°F. During the last stage of that test, thermal cracking occurred in the 1/4" tubing line at 450°F and steam leaked. The system was shut off immediately. As shown in Table 33, the corrosion rate is considerable. MHLB31-MHLB32 was 92.748 mpy, HLB31-HLB32 was 81 mpy. MHLB31 and MHLB32 describe the mag-corrosion cell at the hot end of the flow loop for mud B_3, coupons 1 and 2. HLB31 and HLB32 describe the hot end of the flow loop for mud B_3, coupons 1 and 2. This indicates that the mag-corrosion test is higher than the linear by 11.466 mpy which is mainly due to the rotational motion of the fluid around the stationary specimen. The corrosion rate (35.561 mpy, CLB31, CLB32) is considerably less than the hot section as shown in Figure 23.

In Group No. III, formulation B_3, 150 gram of sea salt and 20 grams caustic soda were added. The corrosion rates, as shown in Table 36 and Figure 24, are considerably

lower than those of group II. The test temperature was increased from 84°F to 400°F for five hours specimen exposure time.

CHAPTER VII

CONCLUSIONS AND RECOMMENDATIONS FOR FUTURE RESEARCH

7.1 Conclusions

In order to monitor the corrosion behavior of drilling fluids at higher temperatures, the fluids must be thermally stable at that condition for a period of time. Thermal stability of different types of mud used in deep drilling and geothermals has been investigated in the laboratory. Sepiolite clay has been added to the testing fluids as a stability controller. The corrosivity of the fluids and environments are studied by measuring the corrosion rate using the weight loss method by three different techniques. The study concluded the following:

1. The stability and rheological properties of the drilling fluids are improved by combining sepiolite clay with bentonite clay in one batch.

2. The corrosion rate of the mud increases as the medium temperature increases if the pH is low and decreases as pH increases, even at high temperature.

3. Thermal breaking of the modified lignosulfonate will allow the multiplication of sulfide-reducing bacteria which reduce the effect of hydrogen sulfide on corrosion and may stop is completely.

4. Corrosion rate varies considerably with the technique used for one drilling fluid. In other words, the corrosion rate measured by the rolling technique is always lower than that measured in the hot end of the flow loop at the same temperature limit. However, it is about equal to that of the cold end of the flow loop.

5. Combining rotational motion with linear motion in one cell (Mag-corrosion) increases the corrosion rate to more than that of the hot end rather than the rolling technique.

6. The static technique gives the lowest corrosion value because in that technique so many factors were eliminated.

7.2 Recommendations for Future Research

Phase I. Corrosion Research

1. Drilling Fluids

a. Different types of corrosion devices, such as flush mounted probes (Petrolite probes) and hydrogen probes, can be incorporated on the mud loop to monitor the corrosion rate continuously. A continuous record of the rate is important because (i) it produces a quick answer as to when, where and to what extent corrosion rate excursions occur, and (ii) to provide a warning when a corrosion rate exceeds a pre-selected maximum value.

b. The temperature limit of 500°F might be increased to 750°F to obtain corrosion data at higher temperatures, especially in geothermal wells. A sand pack can be used with a special experimental set up as a medium to increase the temperature to that limit successfully.

c. Study the effect of direct contamination of acid gases with variable amounts at the bottomhole conditions on the metal corrosion. Consequently, metallurgical investigations to evaluate the ability of the present materials to withstand the effect of these conditions could be undertaken. We would rather recommend additional work on the chemistry of the drilling fluids to develop new chemical additives to minimize corrosion.

2. Oil and Gas Production Processes:

Corrosion study and research should cover oil and gas production, primary under natural forces, secondary and tertiary recovery techniques. These processes will include water flooding, thermal recovery, chemical recovery and also the newly-developed combination processes such as steamo-chemical, foam carbon dioxide, and carbon dioxide steam injection.

Phase 2. Rheology and Stability of Fluids Using the Flow Loop

These fluids which are being widely used in the oil industry can be classified according to the type of operation as follows:

1. Drilling and Packer fluids
2. Hydraulic fracture fluids
3. Micellar and chemically treated slugs used in secondary and tertiary recovery techniques.

Temperature, pressure and shearing limits of these fluids according to the type and condition of operation needs much improvement. The PGE flow loop attached to one of the tertiary recovery techniques can be modified to measure the stability and the limits of all factors encountered in a particular process. These kinds of research are valuable in order to avoid the thermal degradation of these expensive and chemically-complicated fluids.

REFERENCES

1. H.E. Bush, R. D. Barbee and J. P. Simpson. "Current Techniques for Combating Drill-pipe Corrosion," API Drilling and Production Practice, pp. 59-69, 1966.
2. W. C. Skelly and Kjellstrand. "The Thermal Degradation of Modified Lignosulfonates in Drilling Mud," The A.P.I. Div. Prod., Houston, Texas, March 1966.
3. Simpson and Barbee. "Corrosivity of Water Base Completion Fluids," Mat. Prot., 6, No. 12, Dec. 1967.
4. Elio Passaglia. "The Economic Effects of Corrosion Research," NACE, Vol. 35, No. 3, March 1979.
5. A. W. McCray and F. W. Cole. "Oil Well Drilling Technology," Univ. of Okla. Press, Norman, Chapter 7, 1976.
6. Bannerman, J. K., and Devis, Neal. "Sepiolite Used for Hot Wells, Deep Drilling," Oil and Gas Jour., Feb. 27, 1978, pp. 145-150.
7. J. W. Pennington. "History of Drilling Technology and Its Prospects," The Drilling Contractor, Dec. 1949.
8. J. C. Swan. Method of Drilling Wells, U.S. Patent Records No. 1,455,010, Oct. 29, 1919.
9. F. N. Speller. "Corrosion Fatigue of Drill Pipe is Cut by the Chemical Treatment of Mud," Oil and Gas J., Nov. 14, 1935.

10. McMaster. "Battelle Reports on Field Survey," The Drilling Contractor, April 15, 1947.

11. W. H. Betz and L. D. Betz. "Inhibition of Drill Pipe Corrosion," Drilling, May (1949).

12. P. D. Thomas. "Straight and Corrosion Fatigue," Drilling (1939).

13. R. S. Grant and H. G. Texter. "Causes and Prevention of Drill Pipe and Tool-Joint Failures," API Drilling and Production Practice, p. 39-48 (1941).

14. A. P. Maradudin. "Drill Pipe, Casing, Tubing, Sucker Rods--Corrosion Failures and Methods of Combating Corrosion," Reprints of Symposium on Sulfide Stress Corcosion Cracking, NACE, Houston, Texas.

15. Behrens, Holman and Cizek. "Techniques of Evaluation of Corrosion of Drilling Fluids," Paper presented at the Southern District API Meeting, March, 1962.

16. J. Perkins, K. J. Graham, G. A. Storm, G. Leumer and R. P. Schack. "Flow Effects on Corrosion of Galvanic Couples in Sea Water," NACE, Vol. 35, No. 1, Jan. 1979.

17. Speller, F. N. Corrosion, Causes and Preventions. McGraw-Hill Book Co., Inc., New York (1951).

18. A. W. Baumgartner. "Microbiological Corrosion--What Causes It and How It Can Be Controlled." SPE Reprint Series No. 2, Waterflooding.

19. Bakhvalov and Turkovskaya. "Corrosion and Protection of Metals." Pergamon Press, Ltd. 1965.

20. Evans, U. R. Jour. Soc. Chem. Indust., 43, 315 T (1924). (It is mentioned by Laque and Copson, "Corrosion Resistance of Metals and Alloys," Second Edition, A. Ch. Soc., Nomograph Series No. 158, page 325.)

21. J. B. Thuren and others. "Determining Temperature Limits of Drilling Fluids," Final Report submitted to Sandia, Contract No. E(40-1)-5218. Jan. 1979.

22. Anti-Corrosion Manual. 1959 edition, published by Corrosion Prevention and Control.

23. ASTM "Standard Method of Total Immersion Corrosion Test of Stainless Steels," A.279-44T.

24. "Standard Recommended Practice for Preparing, Cleaning, and Evaluating Corrosion Test Specimen," RP 2329, 1970.

25. API, RP 13B; Standard Procedure for Testing Drilling Fluids, page 32.

APPENDIX A

FORMULAE USED

APPENDIX A

FORMULAE USED

A-1. Calculation of Corrosion Rate

a. The corrosion rate in mils per year may be calculated by the following formula:

$$mpy = \frac{\text{weight loss, mg}}{\underset{(gr/cm^3)}{\text{specific gravity}} \times 16.387 \times \underset{(cm^3/in^3)}{\text{area}} \times \underset{(in^2)}{\text{time, year}} \quad \underset{(days/365)}{}}$$

The mild steel coupons used in this study have a specific gravity equal to 7.86 gr/cm^3; thus this formula may be reduced to:

$$mpy = \frac{68.33 \times \text{weight loss, mg}}{\text{area } (in^2) \times \text{hours of exposure}} \qquad \text{(A-1)}$$

b. The corrosion rate in kilograms per square meter per year may be calculated by the following formula:

$$kg/m^2/yr = \frac{\text{wt. loss, mg}}{1{,}000{,}000} \times \frac{10{,}000}{\text{area, } cm^2} \times \frac{365}{\text{days of exposure}}$$

$$= \frac{\text{wt. loss, mg} \times 87.60}{\text{area, } cm^2 \times \text{hours exposed}}$$

$$kg/m^2/yr = \frac{\text{wt. loss, mg} \times 13.58}{\text{area, } in^2 \times \text{hours exposed}} \qquad \text{(A-2)}$$

c. The corrosion rate in pounds per square foot per year may be calculated by the following formula:

$$lb/ft^2/ys = \frac{\text{wt. loss, mg}}{453{,}600} \times \frac{144}{\text{area, in}^2} \times \frac{365}{\text{days exposure}}$$

$$= \frac{\text{wt. loss, mg} \times 2.781}{\text{area, in}^2 \times \text{hours exposed}} \qquad \text{(A-3)}$$

A-2. Corrosion Rate Unit Conversions

The following are the conversion rates between the various units for steel coupons (specific gravity, 7.86).

$mpy = 24.62 \times lb/ft^2/yr$

$mpy = 5.03 \times kg/m^2/yr$

$lb/ft^2/yr = 0.04 \times mpy$

$lb/ft^2/yr = 0.20 \times kg/m^2/yr$

$kg/m^2/yr = 0.20 \times mpy$

$kg/m^2/yr = 4.90 \times lb/ft^2/yr$

Equation (A-1) is used in the calculation of the corrosion rate in this study.

APPENDIX B

TABLES AND ILLUSTRATIONS

Mud Composition

Bentonite + Water + Sodium Chloride

Rheological Properties:

Initial Gel, $lb/100ft^2$	14
Plastic viscosity, cp	7
($\phi_{600} = 32$, $\phi_{300} = 25$)	
Yield Point, $lb/100\ ft^2$	18
Mud Weight, lb/gal	8.62
pH	9/10.0

Corrosion Data:

Material: Mild Steel 1018	
Test Temperature, °F	200
Time of Exposure, hrs	21.5

Table 1: Corrosion Test

Rolling Test (Temperature 200°F)

Mud Type: Saline Commercial Mud

1	2	3	4	5	6	7	8	9	10	11	12
Test Number	Cell	Specimen	pH	Mud Weight PPG	Area in^2	Coupon Weight Before gram	Coupon Weight After gram	Weight Loss mg	Time of Exposure hrs	Corrosion Rate mpy	Average Corrosion Rate mpy
1	A	R_1	9	8.62	1.6	6.3330	6.3100	23.0	21.5	45.686	58.1
	A	R_2	9	8.62	1.6	6.4003	6.3650	35.3	21.5	70.515	
2	C	R_1	10	8.62	1.6	6.2030	6.1900	13.0	21.5	21.06	23.44
	C	R_2	10	8.62	1.6	6.1550	6.1440	11.0	21.5	25.822	

Mud Components:

1. Bentonite Clay
2. Barite
3. Calcium Chloride
4. Polymer

Rheological Properties:

Initial Gel, lb/100 ft^2	20
Plastic Viscosity, cp	36
(ϕ_{600} = 87, ϕ_{300} = 51)	
Yield Point, lb/100 ft^2	15
Mud Weight, lb/gal	8.88
pH	9/10.5

Corrosion Data:

Material: Mild Steel 1018	
Test Temperature, °F	300
Time of Exposure, hrs	24

Purpose of the Test: Effect of caustic soda (pH) on corrosion rate for potassium chloride, polymer base mud

Table 2: Corrosion Test

Rolling Test (Temperature 300°F)

Mud Type: Plymer (Salt Water base mud)

1	2	3	4	5	6	7	8	9	10	11	12
Test Number	Cell	Specimen	pH	Mud Weight PPG	Area in^2	Coupon Weight Before gram	Coupon Weight After gram	Weight Loss mg	Time of Exposure hrs	Corrosion Rate mpy	Average Corrosion Rate mpy
3	A	R_1	9	8.88	1.6	6.2650	6.2450	20.0	24	35.588	40.927
	A	R_2	9	8.88	1.6	5.9920	5.9660	26.0	24	46.265	
4	C	R_1	10.5	8.88	1.6	6.1550	6.1450	10.0	24	17.794	22.243
	C	R_2	10.5	8.88	1.6	6.3100	6.2950	15.0	24	26.691	

Schedule of the Rolling Tests

Mud Type	B_1	B_2	B_3
Temperature Range (°F)	200	200	200
	300	300	300
	400	400	400
	500	500	500
pH (Constant)	7.67	Change	

Table 3: Corrosion Test

Rolling Test (Temperature 200°F)

A-RB1-200; Mud B_1

1	2	3	4	5	6	7	8	9	10	11	12
Test Number	Cell	Specimen	pH	Mud Weight PPB	Area in^2	Coupon Weight Before gram	Coupon Weight After gram	Weight Loss mg	Time of Exposure hrs	Corrosion Rate mpy	Average Corrosion Rate mpy
5	A	R_1	7.67	476.9	2.531	9.4155	9.3860	29.5	24	33.184	26.519
	A	R_2	7.67	47.69	2.531	9.4665	9.4490	17.5	24	19.854	

Table 4: Corrosion Test

Rolling Test (Temperature 300°F)

A-RB1-300; Mud B_1.

1	2	3	4	5	6	7	8	9	10	11	12
Test Number	Cell	Specimen	pH	Mud Weight PPB	Area in^2	Coupon Weight Before gram	Coupon Weight After gram	Weight Loss mg	Time of Exposure hrs	Corrosion Rate mpy	Average Corrosion Rate mpy
6	A	R_1	7.67	476.9	2.53	9.7652	9.5940	171.2	31	149.153	150.373
	A	R_2	7.67	476.9	2.53	9.8075	9.6335	174.0	31	151.593	

Table 5: Corrosion Test

Rolling Test (Temperature 400°F)

A-RB1-400; Mud B_1

1	2	3	4	5	6	7	8	9	10	11	12
Test Number	Cell	Specimen	pH	Mud Weight PPB	Area in^2	Coupon Weight Before gram	Coupon Weight After gram	Weight Loss mg	Time of Exposure hrs	Corrosion Rate mpy	Average Corrosion Rate mpy
7	A	R_1	7.67	476.9	2.53	9.5940	9.4715	122.5	16	206.779	202.137
	A	R_2	7.69	476.9	2.53	9.6335	9.5165	117.0	16	197.495	

Note: The coupons used for test No. is that of Test No. rolling and the same drilling fluid has been used after stirring for 5 min.

Table 6: Corrosion Test

Rolling Test (Temperature 500°F)

A-RB1-500; Mud B_1

1	2	3	4	5	6	7	8	9	10	11	12
Test Number	Cell	Specimen	pH	Mud Weight PPB	Area in^2	Coupon Weight Before gram	Coupon Weight After gram	Weight Loss mg	Time of Exposure hrs	Corrosion Rate mpy	Average Corrosion Rate mpy
8	A	R_1	7.67	476.9	2.531	9.4715	9.4155	56.0	23.75	63.657	60.247
	A	R_2	7.67	476.9	2.531	9.5165	9.4665	50.0	23.75	56.836	

Table 7: Corrosion Test

Rolling Test (Temperature 200°F)

C-RB1-200

1	2	3	4	5	6	7	8	9	10	11	12
Test Number	Cell	Specimen	pH	Mud Weight PPB	Area in^2	Coupon Weight Before gram	Coupon Weight After gram	Weight Loss mg	Time of Exposure hrs	Corrosion Rate mpy	Average Corrosion Rate mpy
9	C	R_1	7.67	476.9	2.531	9.6385	9.6045	34.0	24	38.246	37.684
	C	R_2	7.67	476.9	2.531	9.6565	9.6235	33.0	24	37.121	

Table 8: Corrosion Test

Rolling Test (Temperature 300°F)

C-RB1-300

1	2	3	4	5	6	7	8	9	10	11	12
Test Number	Cell	Specimen	pH	Mud Weight PPB	Area in^2	Coupon Weight Before gram	Coupon Weight After gram	Weight Loss mg	Time of Exposure hrs	Corrosion Rate mpy	Average Corrosion Rate mpy
10	C	R_1	7.67	476.9	2.531	9.6045	9.4105	194	31	169.950	167.273
	C	R_2	7.67	476.9	2.531	9.6235	9.4345	189	31	164.596	

Table 9: Corrosion Test

Rolling Test (Temperature 400°F)

C-RB1-400

1	2	3	4	5	6	7	8	9	10	11	12
Test Number	Cell	Specimen	pH	Mud Weight PPB	Area in^2	Coupon Weight Before gram	Coupon Weight After gram	Weight Loss mg	Time of Exposure hrs	Corrosion Rate mpy	Average Corrosion Rate mpy
11	C	R_1	7.67	476.9	2.531	9.3860	9.2700	116	24	130.487	126.550
	C	R_2	7.67	476.9	2.531	9.4490	9.3400	109	24	122.612	

Table 10: Corrosion Test

Rolling Test (Temperature 500°F)

C-RB1-500

1	2	3	4	5	6	7	8	9	10	11	12
Test Number	Cell	Specimen	pH	Mud Weight PPB	Area in^2	Coupon Weight Before gram	Coupon Weight After gram	Weight Loss mg	Time of Exposure hrs	Corrosion Rate mpy	Average Corrosion Rate mpy
12	C	R_1	7.67	476.9	2.531	9.4105	9.1990	211.5	32 *54	178.435 *105.739	
	C	R_2	7.67	476.9	2.531	9.4345	9.2125	222	32 *54	187.29 *110.988	

*The cell was actually under test for 54 hrs, 18 hrs under 400°F and rolling, 14 hrs under 500°F and rolling, and 22 hrs at room temperature and static conditions.

The corrosion rates of 178.435 and 187.29 are right only if we neglect the corrosion behavior of the mud at room temperature and static conditions which is incorrect.

Table 11

Summary of the Results

Rolling Technique

Cells A & C; Mud B_1

Technique/ Fluid	Mud Wt PPB	pH	Temp °F	C. R. av. mpy Cell A	Cell C
RB1	476.9	7.67	200	26.519	37.684
RB1	476.9	7.67	300	150.373	167.273
RB1	476.9	7.67	400	202.137	126.66
RB1	476.9	7.67	500	60.247	108.364* 188.863**

*Average corrosion rate due to the effect of the two techniques for a time of exposure of 54 hours.

**Average corrosion rate considering only the effect of the rolling technique and neglecting the effect of the static technique at room temperature for a period of 22 hours.

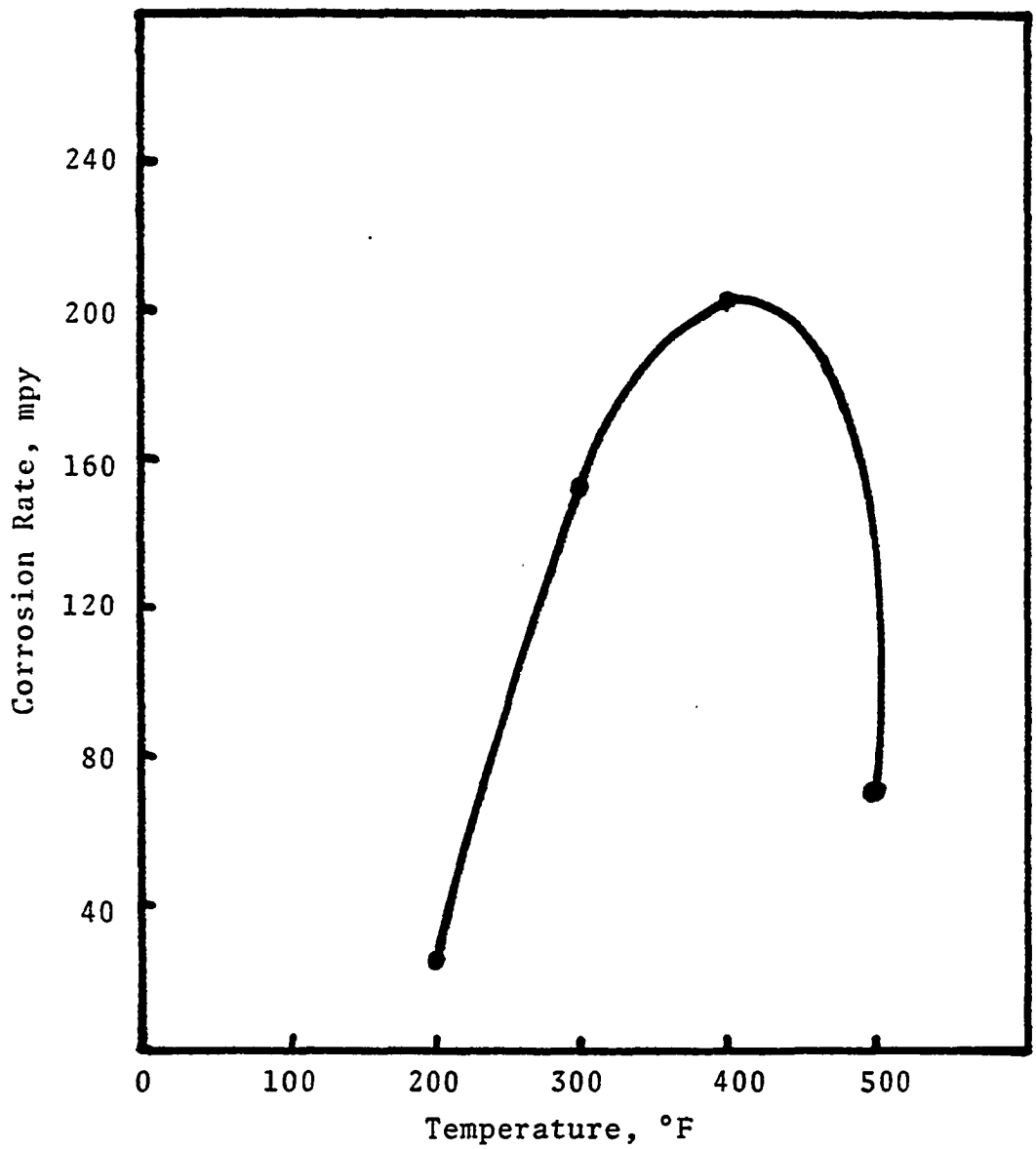


Figure 11: Corrosion rate as a function of temperature for mud B_1, constant pH, cell A.

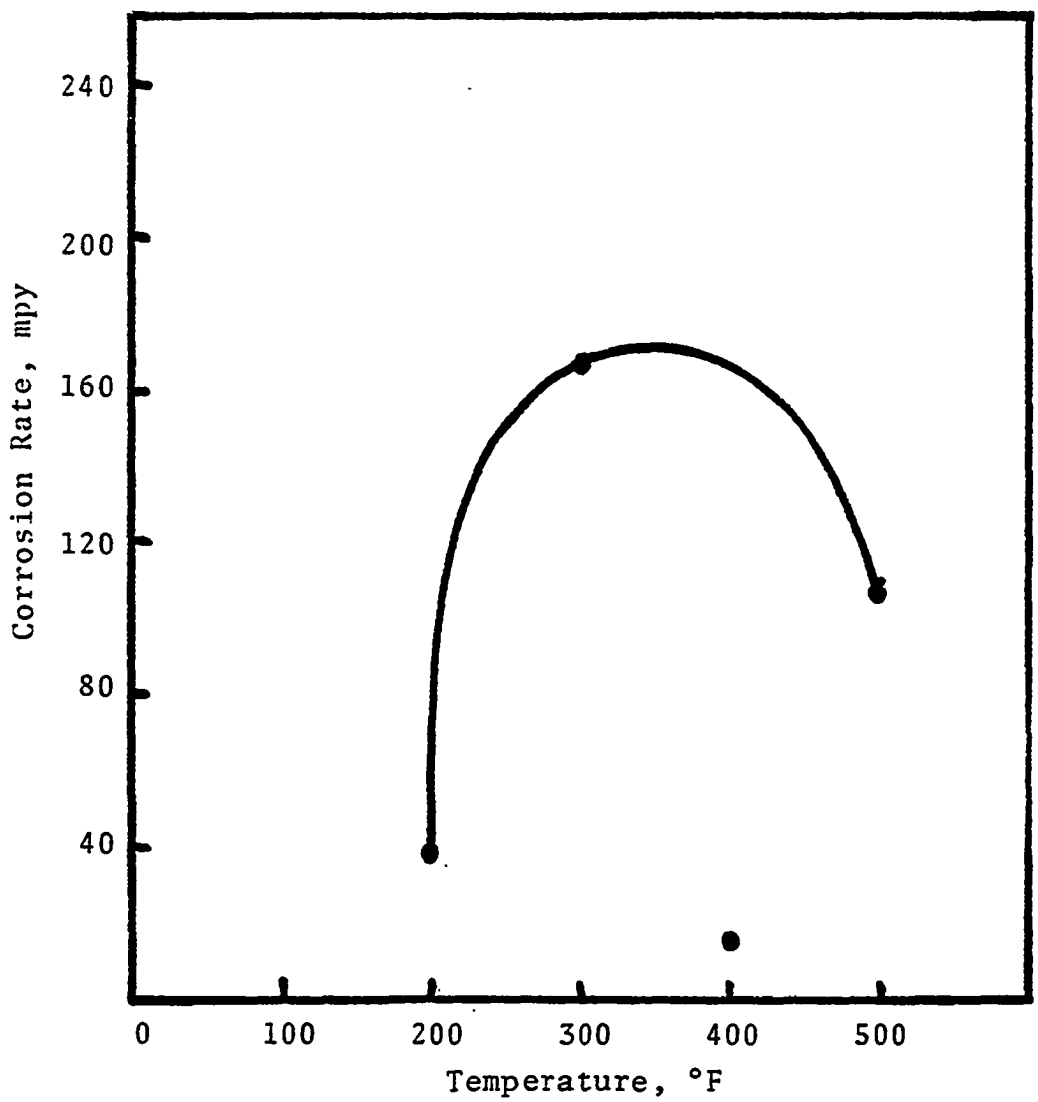


Figure 12: Corrosion rate as a function of temperature for mud B_1, constant pH, cell C.

Table 12

B_1 Mud Stability Test Using Sandia-Lab Flow Loop

Time When Taking Reading	Pressure Differential psiD			Pressure Absolute psi		Temperature °F	Flow Rate cm^3/sec	pH
	ΔP 1/4"/psi	ΔP 3/8"/psi	ΔP 5/8"/psi	P_{in}	P_{out}			
3:00	0.95	0.09	0.02	1350	1250	400	0.862	9.81
3:30	0.90	0.12	0.03	1300	1250	400	0.862	9.61
4:00	0.85	0.15	0.02	1250	1100	400	0.862	9.56
4:30	0.82	0.07	2.02	1350	1300	400	0.862	9.34
5:00	0.83	0.09	0.03	1200	1100	400	0.984	9.50
5:30	0.83	0.11	0.03	1300	1150	450	0.984	9.66
6:00	0.85	0.10	0.03	1250	1150	450	0.962	9.69
6:30	0.88	0.12	0.02	1280	1180	450	0.962	9.72

Test No. 13

Table 13

Corrosion Test: Sandia-Lab Flow Loop, Tap Water, 24 Hours Agins

1	2	3	4	5	6	7	8	9	10	11	12
Test Number	Loop End	Specimen	pH	Mud Weight PPB	Area in^2	Coupon Weight Before gram	Coupon Weight After gram	Weight Loss gram	Time of Exposure hrs	Corrosion Rate mpy	Average Corrosion Rate mpy
14	Hot	LH-1	9.81	511	2.53	9.6896	9.6606	0.0285	3	256.575	253.424
	Hot	LH-2	9.81	511	2.53	9.8426	9.7646	0.0278	3	250.273	
15	Cold	LC-1	9.81	511	2.53	9.7565	9.7386	0.0179	3	161.147	155.746
	Cold	LC-2	9.81	511	2.53	9.7976	9.7816	0.0167	3	150.344	

Test Conditions:

1. Temperature 400°F 450°F
2. Exposure time 2 hrs 1 hr
3. Cold end 110°F 3 hrs (Total exposure time at the cold end)

Remarks: (a) Corrosion rate at the hot end is much higher than the cold end.
(b) Corrosivity of that fluid is severe at high temperature.

Recommendations: Drill pipes should be replaced every year or less.

Table 14: Corrosion Test

Rolling Test, 24 hours Aging Time

1	2	3	4	5	6	7	8	9	10	11	12
Test Number	Cell	Specimen	pH	Mud Weight PPB	Area in^2	Coupon Weight Before gram	Coupon Weight After gram	Weight Loss mg	Time of Exposure hrs	Corrosion Rate mpy	Average Corrosion Rate mpy
16	A	R1	9.81	511	2.53	9.8216	9.8067	14.9	2.67	150.718	157.799
	A	R2	9.81	511	2.53	9.7983	9.7820	16.3	2.67	164.880	

Mud Type B_1

Mud Aged for 24 hrs.

Temperature raised directly to 400°F and 450°F (Sudden exposure)

Table 15

Corrosion Test: Flow Loop
Distilled Water, No Aging

1	2	3	4	5	6	7	8	9	10	11	12
Test Number	Loop End	Specimen	pH	Mud Weight PPB	Area in^2	Coupon Weight Before gram	Coupon Weight After gram	Weight Loss mg	Time of Exposure hrs	Corrosion Rate mpy	Average Corrosion Rate mpy
17	Hot	LH-1	11	510	2.579	9.7326	9.7218	10.8	2.67	107.170	110.643
	Hot	LH-2	11	510	2.579	9.6589	9.6474	11.5	2.67	114.116	
18	Cold	LC-1	11	510	2.579	9.6964	9.6946	1.8	2.67	17.86	20.838
	Cold	LC-2	11	510	2.579	9.7056	9.7032	2.4	2.67	23.816	

More Information:

1. Temp. °F: 200 300 400 480
2. Time, min: 35 40 45 40
3. Cold End Temp. °F: 110
4. Steam leak at 2 connections in the test section, system was shut off, Fig. 25
5. Distilled water

Table 16

Corrosion Test: Rolling

1	2	3	4	5	6	7	8	9	10	11	12
Test Number	Cell	Specimen	pH	Mud Weight PPB	Area in^2	Coupon Weight Before gram	Coupon Weight After gram	Weight Loss mg	Time of Exposure hrs	Corrosion Rate mpy	Average Corrosion Rate mpy
19	A	R_1	11	511	2.53	9.6435	9.6420	1.5	2.67	14.819	15.807
	A	R_2	11	511	2.53	9.6575	9.6558	1.7	2.67	16.795	

Mud Type: B_1

Distilled Water

Fresh Sample

Temperature increased gradually

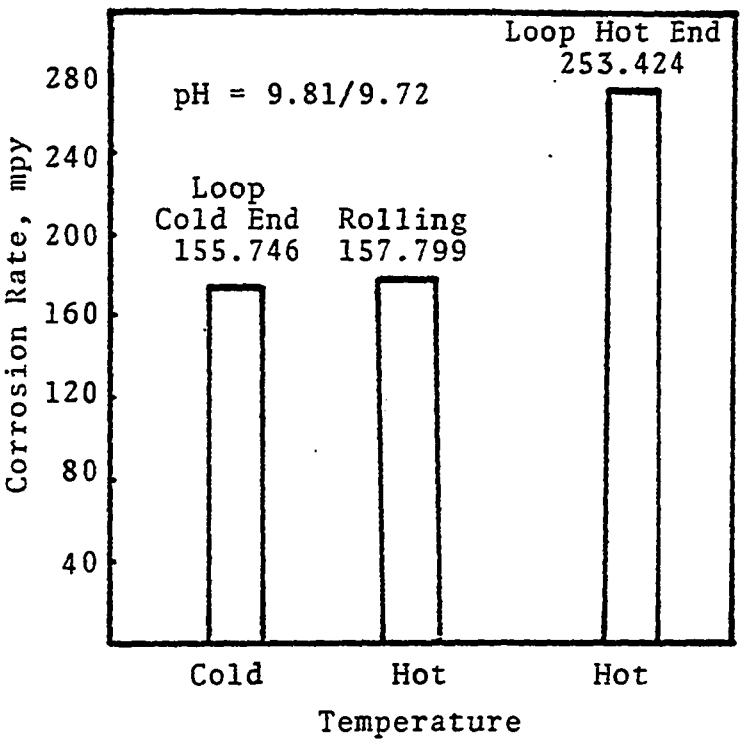


Figure 13: Bar diagram corrosion rate vs. temperature °F (Tap water, 24 hr. aging, and mode of change)

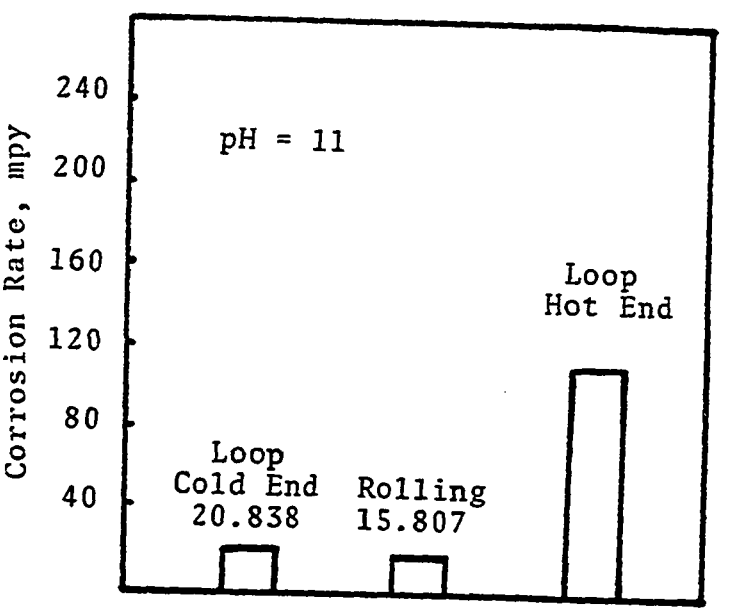


Figure 14. Bar diagram corrosion rate v.s temperature °F (Distilled water, fresh fluid, and gradual change in temperature).

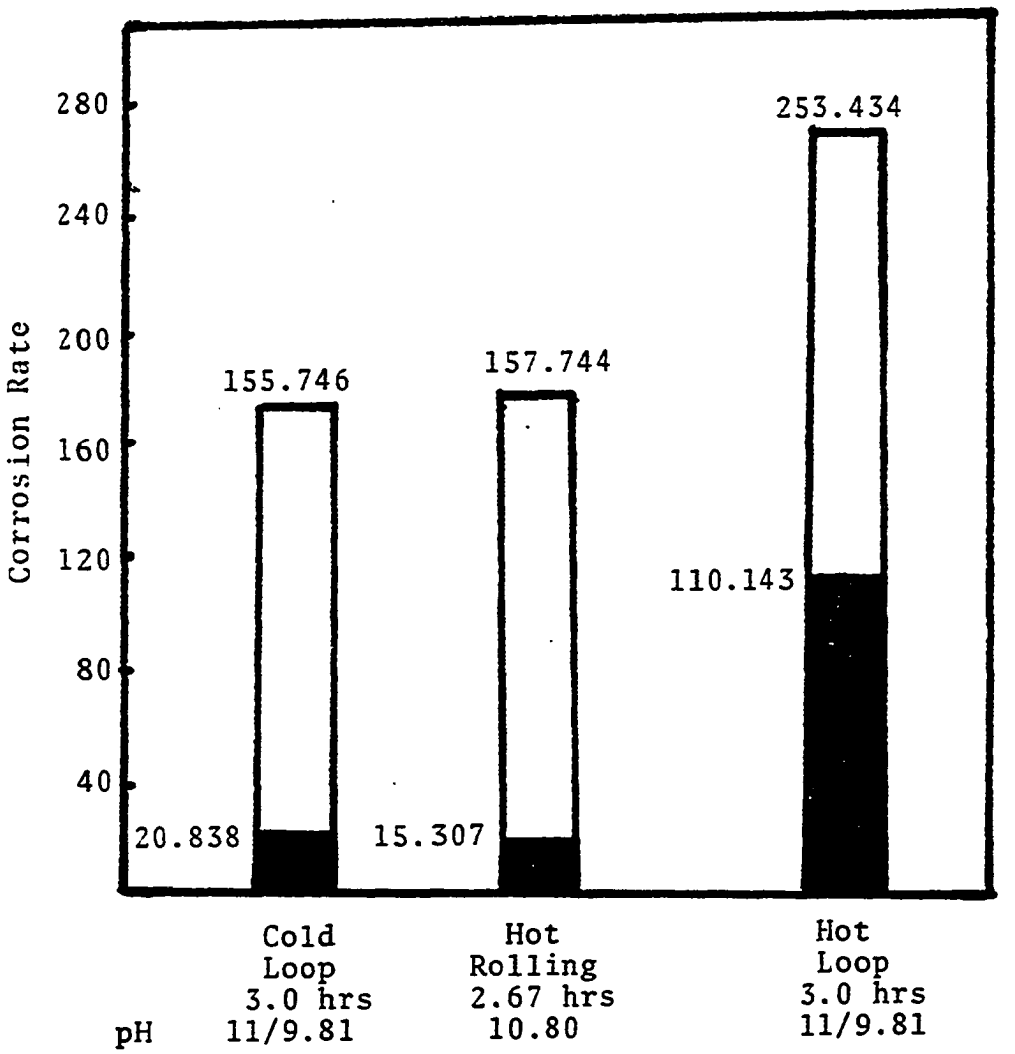


Figure 15: Bar diagram, correlation between techniques, flow loop and rolling.

Type of Mud: B_1

Mud Composition:

Bentonite

Sepiolite

Lignite

Caustic Soda

Tap Water

Mud Characteristics:

Mud pH	10.45
Plastic Viscosity, cp	4.5

Test Material: Mild Steel (1018)

Test Conditions:

Temperature, °F	80	200	300	350
*pH	10.45	9.92	9.12	8.76
Time, hrs	2	1	1	1

*pH value measured instantaneously by Orion digital pH meter. As shown in Figure 16, the pH value of the mud decreases with temperature and to maintain pH constant, addition of a concentrated solution of caustic soda is needed.

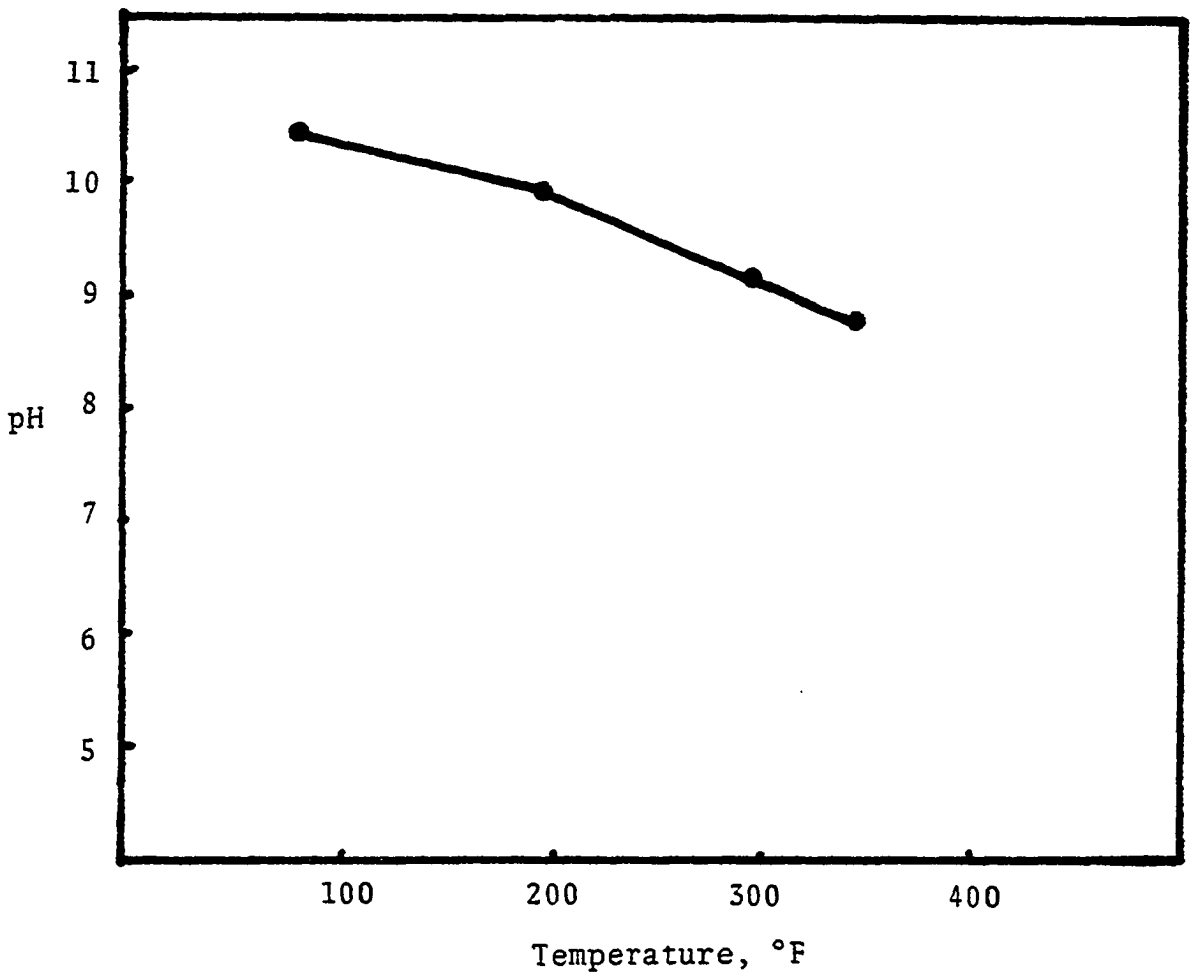


Figure 16: Effect of temperature on pH for drilling fluid.

Table 17

Corrosion Test: Sandia-Lab Flow Loop

Mud Type: B_1

1	2	3	4	5	6	7	8	9	10	11	12
Test Number	Loop End	Specimen	pH	Mud Weight PPB	Area in^2	Coupon Weight Before gram	Coupon Weight After gram	Weight Loss mg	Time of Exposure hrs	Corrosion Rate mpy	Average Corrosion Rate mpy
20	Hot	LH-1	10.45	511	2.519	9.7430	9.7385	4.5	5	23.899	21.778
	Hot	LH-2	10.45	511	2.519	9.7185	9.7148	3.7	5	19.655	
21	Cold	LC-1	10.45	511	2.519	9.7012	9.6992	2.0	5	10.622	11.684
	Cold	LC-2	10.45	511	2.519	9.7862	9.7238	2.4	5	12.746	

Test Conditions:

Temperature, °F	80	200	300	350
Time of Exposure, hrs	2	1	1	1

Table 18

Corrosion Test: Rolling

Type of Mud: B_1

1	2	3	4	5	6	7	8	9	10	11	12
Test Number	Cell	Specimen	pH	Mud Weight PPB	Area in^2	Coupon Weight Before gram	Coupon Weight After gram	Weight Loss mg	Time of Exposure hrs	Corrosion Rate mpy	Average Corrosion Rate mpy
22	A	R_1	10.45	511	2.53	9.6869	9.6839	3.0	5	15.933	14.871
	A	R_2	10.45	511	2.53	9.6740	9.6714	2.6	5	13.808	

Table 19: Corrosion Test

PGE Flow Loop: Temperature* ≈ 250°F

1	2	3	4	5	6	7	8	9	10	11	12
Test Number	Loop End	Specimen	pH	Mud Weight PPB	Area in^2	Coupon Weight Before gram	Coupon Weight After gram	Weight Loss mg	Time of Exposure hrs	Corrosion Rate mpy	Average Corrosion Rate mpy
23	Hot	LH-1	10.27	465.2	2.53	9.6830	9.6801	2.9	3.1	25.267	26.136
	Hot	LH-2	10.27	465.2	2.53	9.6898	9.6867	3.1	3.1	27.000	
24	**Cold	LC-1	10.27	465.2	2.53	9.6748	9.6735	1.3	3.1	11.326	12.197
	Cold	LC-2	10.27	465.2	2.53	9.7547	9.7532	1.5	3.1	13.068	

· The fluid at the hot end rotates in the Magcorrosion cell

* The temperature is an average because the controllers were not wired yet.

** The ambient temperature measured by thermocouple thermometer

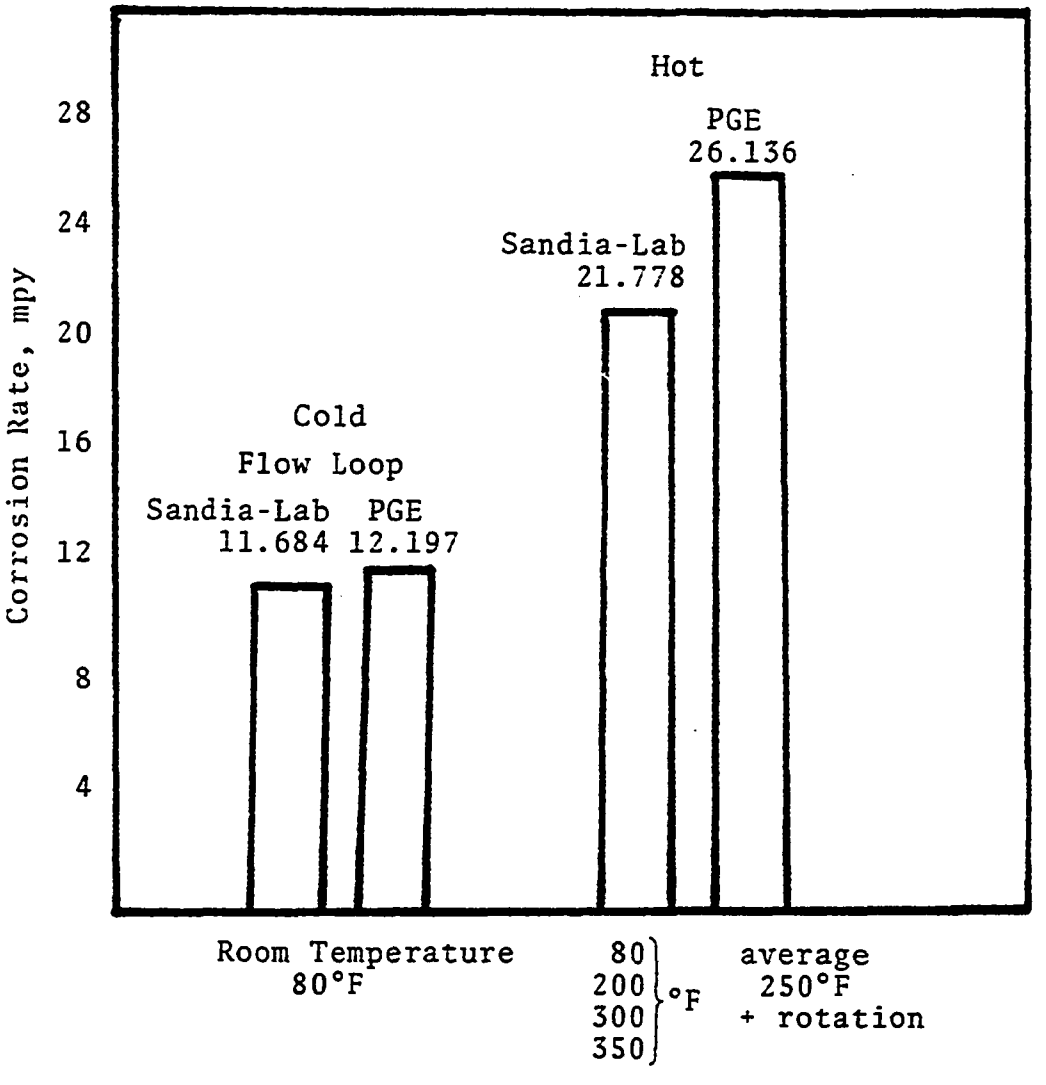


Figure 17: Bar diagram to show equal efficiency of PGE and Sandia-Lab flow loops to measure the corrosion rate.

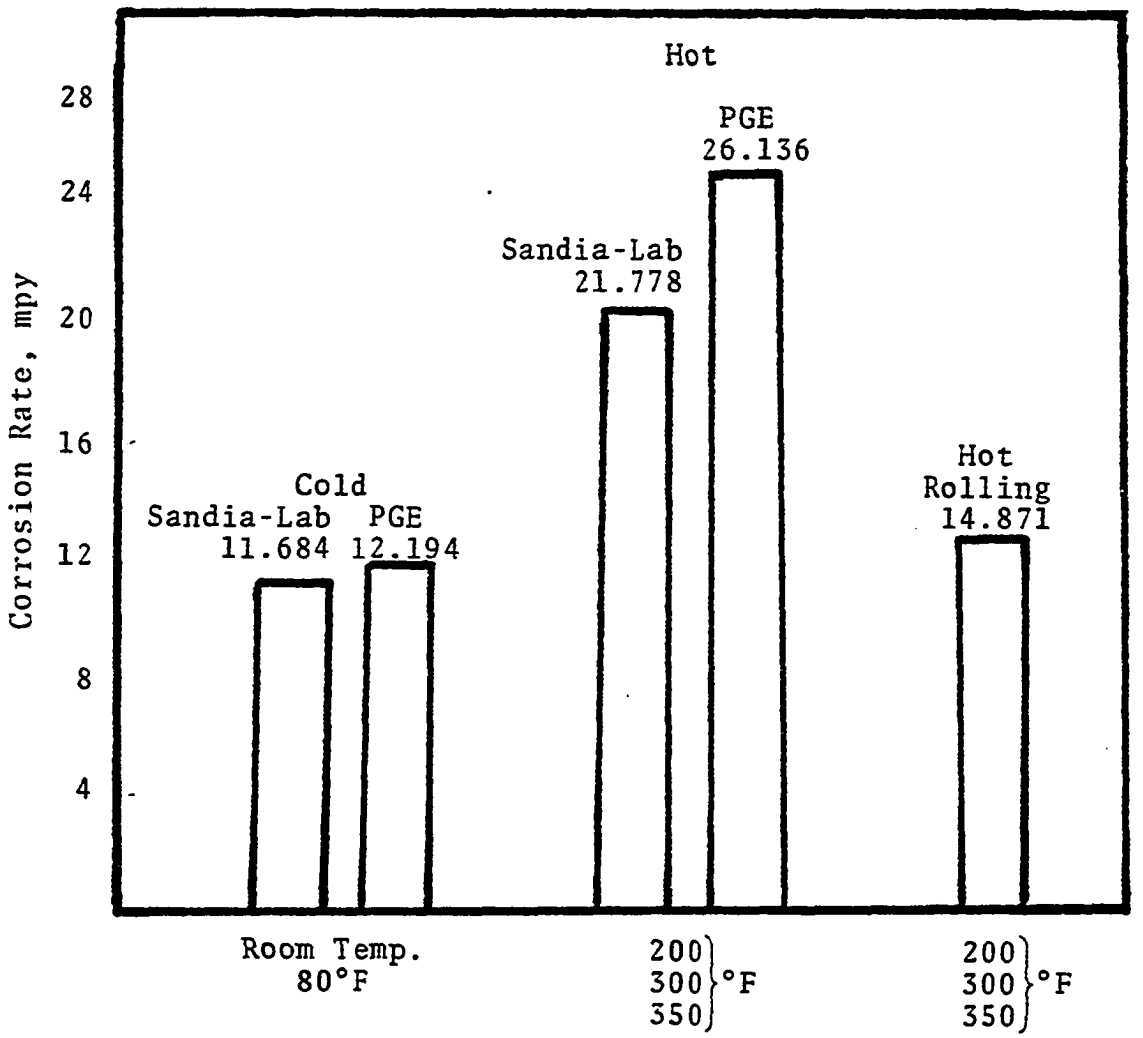


Figure 18: Combination of the two techniques (flow loop and rolling)

Table 20

Sandia-Lab Flow Loop Test: Rheology and Stabilization Test

Test No.	Time	Temp °F	*Rheological Properties: Initial Gel lb/100 ft²	10 min. Gel lb/100 ft²	ϕ_{600}	ϕ_{300}	PV cp	Yield lb/100 ft²	Flow Rate cc/sec	pH	Flow Loop Reading (psi): Δp 1/4"	Δp 3/8"	Δp 5/8"	P_{in} psi	P_{out} psi	Remarks
1	10:30	R.T.	3	-	-	-	-	-	-	-	0.8	0.71	0.3	600	520	(1)
2	10:45	R.T.	2	-	3	6.5	3.5	3.0	-	10.94	1.2	0.3	0.3	800	650	(2)
3	11:00	R.T.	2	3	6	4	2	2.0	-	10.95	2.6	0.24	0.25	800	650	(3)
4	11:50	-	-	-	-	-	-	-	-	-	-	-	-	-	-	
5	12:15	200	1.0	2	5	3	2	1.0	14.7	10.88	2.7	0.03	0.3	930	870	
6	1:15	200	1	1	4.5	2.5	2	0.5	14.7	10.75	1.32	0.05	0.3	980	890	
7	2:15	200	1	1	6	3.5	2.5	1.0	13.7	10.93	1.28	0.1	0.3	930	850	
8	3:15	200	1	1	7	5	2	3	14.0	10.92	1.30	0.8	0.3	910	820	
9	4:15	200	1	-	8	5	3	2	-	10.91	1.31	0.06	0.35	800	700	(4)
10	5:15	300	1	2.5/1.0	10	6	4	2	14.2	10.8	1.74	0.5	0.18	1200	1150	
11	6:15	300	14/11	35/16	23	20	3	17	14.0	10.72	4.66	1.94	0.13	1400	1375	
12	6:30	350	10	45/18	21.5	18	3.5	14.5	14.4	10.66	4.22	5.23	0	1200	1175	
13	6:45	350	10/9	40/15	21	17	4	13	13.3	10.66	3.70	2.1	0.2	1375	1300	(5)
14	7:15	350	37/16	70/21	31	27	4	23	7.7	10.66	2.90	2.1	0.2	1000	900	

(1) water circulating (2) feed pressure 17 psi (3) Pressure change from 600 to 1100 psi
(4) fluid started jelling (5) fluctuating

Comments:
Beginning water flush at ambient temperature
Test stopped at 8:00 p.m.: Running time - 9 ½ hrs
The system has no plugging problem at all.
*Rheological properties measured by V.G. Baroid rheometer

Table 21: Corrosion Test

Sandia-Lab Flow Loop Corrosion Test: Mud B_1

1	2	3	4	5	6	7	8	9	10	11	12
Test Number	Loop End	Specimen	pH	Mud Weight PPB	Area in^2	Coupon Weight Before gram	Coupon Weight After gram	Weight Loss mg	Time of Exposure hrs	Corrosion Rate mpy	Average Corrosion Rate mpy
26	Hot	LH-1	10-11	388.06	2.494	9.7200	9.7113	8.70	9.5	25.05	20.008
	Hot	LH-2	10-11	388.06	2.499	9.6420	9.6368	5.20	9.5	14.97	
27	Cold	LC-1	10-11	388.06	2.499	9.7706	9.7660	4.6	9.5	13.240	13.816
	Cold	LC-2	10-11	388.06	2.499	9.7330	9.7280	5.0	9.5	14.391	

Table 22: Corrosion Test

Rolling Test: Mud B_1

28	*Rol	AR-1	10.5	388.06	2.562	9.8033	9.8000	3.3	6	14.668	13.78
	**Rol	AR-2	10.5	388.06	2.562	9.6807	9.6778	2.9	6	12.891	

*2¼ hours at 200°F

**3.75 hours at 300°F

Table 23: Corrosion Test

Static Corrosion Test: Mud B_1

1	2	3	4	5	6	7	8	9	10	11	12
Test Number	Test Temp °F	Specimen	pH	Mud Weight PPB	Area in^2	Coupon Weight Before gram	Coupon Weight After gram	Weight Loss mg	Time of Exposure hrs	Corrosion Rate mpy	Average Corrosion Rate mpy
29	200	ASB11	10.58	388.06	2.562	9.8172	9.8134	3.8	24	4.321	3.769
	300	ASB12	10.58	388.06	2.562	9.7953	9.7924	2.8	24	3.217	

Time of exposure at each temperature: 12 hours

Table 24

Rheological Data

(1) Temperature °F	(2) Flow Rate cc/sec	(3) Pressure In/Out psi	(4) P.V. cp	(5) No. of Tests
R.T.	14.700	930/870	2.75	2
200	14.275	922.5/857.5	2.30	5
300	14.100	1300/1262.5	3.50	2
350	11.800	1191.7/1125	3.83	3

*Plastic viscosity has been determined by Baroid Rheometer.

Corrosion Data

1 - Flow Loop

a. Hot Cell, average corrosion rate = 20.008 mpy

b. Cold cell, average corrosion rate = 13.816 mpy

2 - Rolling

Average corrosion rate = 13.78 mpy

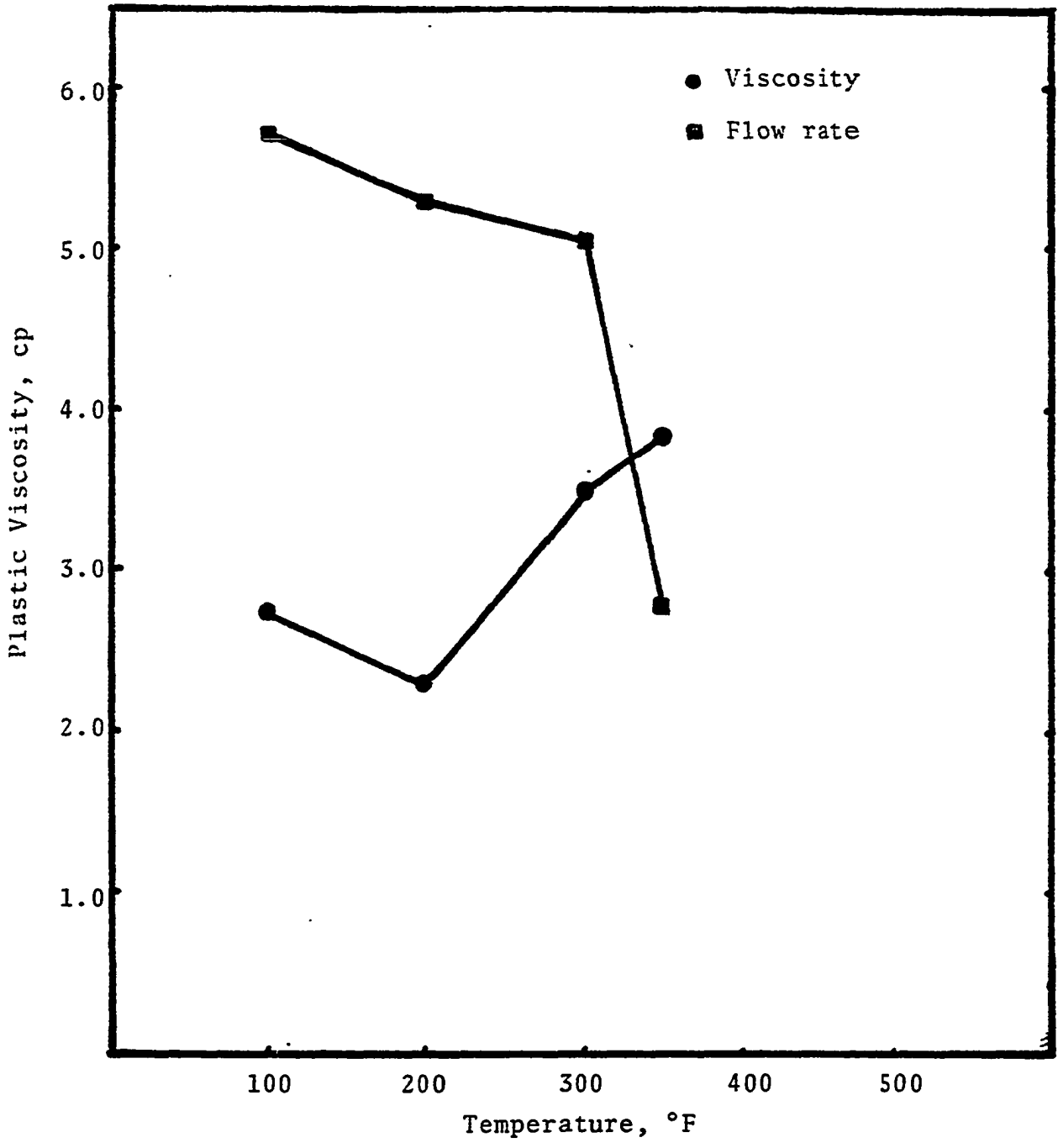


Figure 19: Effect of temperature on plastic viscosity, cp, and flow rate, cc/sec.

Fig 19

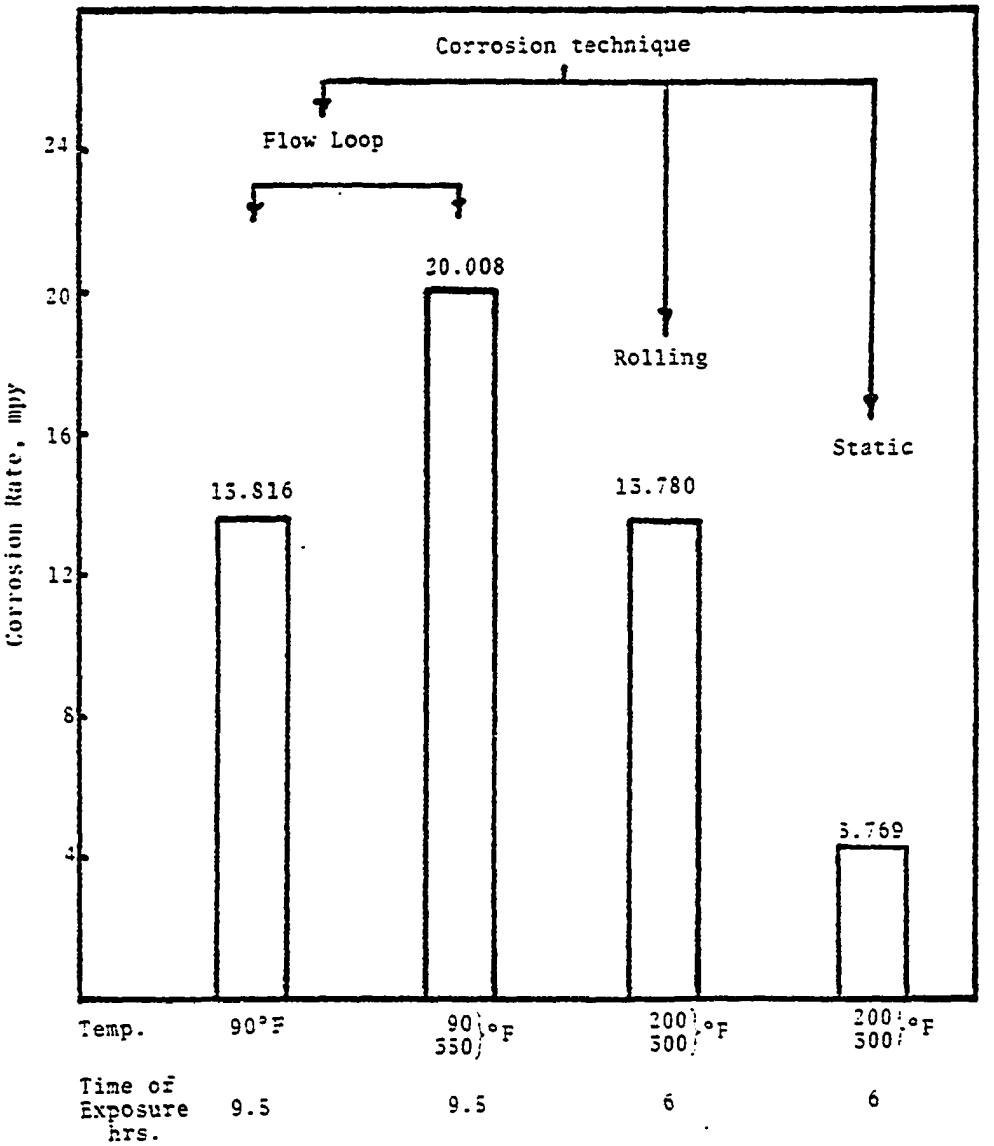


Figure 20: Bar diagram to show the relationship between corrosion techniques (flow loop, rolling and static)

Mud B_2

Formulation:

80 grams	Resinex
30 grams	Bendonite
30 grams	Sepiolite
5 grams	Sea Salt
7 grams	Caustic soda
1000 cc	Tap water

Physical Properties from Baroid Rheometer

Mud Weight	404.8 lb/bbl
pH	10.13-10.68
Plastic viscosity	5 cp
Yield point	35 lb/100 ft^2
Gels, initial	17 lb/100 ft^2
Gel, 10 minutes	--

Test temperature - 300°F after rolling test for 24 hours.

Table 25: Corrosion Test

Rolling Test (Temperature 200°F)

Mud B_2 A-RB2-200

1	2	3	4	5	6	7	8	9	10	11	12
Test Number	Cell	Specimen	pH	Mud Weight PPB	Area in^2	Coupon Weight Before gram	Coupon Weight After gram	Weight Loss mg	Time of Exposure hrs	Corrosion Rate mpy	Average Corrosion Rate mpy
29	A	R_1	10.68	404.8	2.53	9.6655	9.6650	0.5	15.5	0.87	0.87
	A	R_2	10.68	404.8	2.53	9.7360	9.7355	0.5	15.5	0.87	negligible

Table 26: Corrosion Test

Rolling Test (Temperature 300°)

A-RB2-300

30	A	R_1	10.20	404.8	2.53	9.6550	9.6650	0	24	0	1.069
	A	R_2	10.20	404.8	2.53	9.7355	9.7336	1.9	24	2.138	negligible

The coupons after the 200 and 300°F tests were very clean with no oxide spots, no change. The fluid was stirred for five minutes before the 300°F test and put back in the rolling oven. The same coupons were used for all runs.

Table 27: Corrosion Test

Rolling Test (Temperature 400°F)

A-RB2-400

1	2	3	4	5	6	7	8	9	10	11	12
Test Number	Cell	Specimen	pH	Mud Weight PPB	Area in^2	Coupon Weight Before gram	Coupon Weight After gram	Weight Loss mg	Time of Exposure hrs	Corrosion Rate mpy	Average Corrosion Rate mpy
31	A	R_1	10.13	404.8	2.53	9.6550	9.6550	0.0	24	0.0	0.849
	A	R_2	10.13	404.8	2.53	9.7335	9.7320	1.5	24	1.688	

Table 28: Corrosion Test

Rolling Test (Temperature 500°F)

A-RB2-500

32	A	R_1	8.25	404.8	2.53	9.6650	9.6580	7.0	24	7.877	5.345
	A	R_2	8.25	404.8	2.53	9.7320	9.7295	2.5	24	2.813	

Drilling Fluid B_2

Mud Weight: 404.8 PPB

Temperature °F	pH	Av. Cor. Rate mpy
200	10.68	0.87
300	10.20	1.069
400	10.13	0.849
500	8.25	5.345

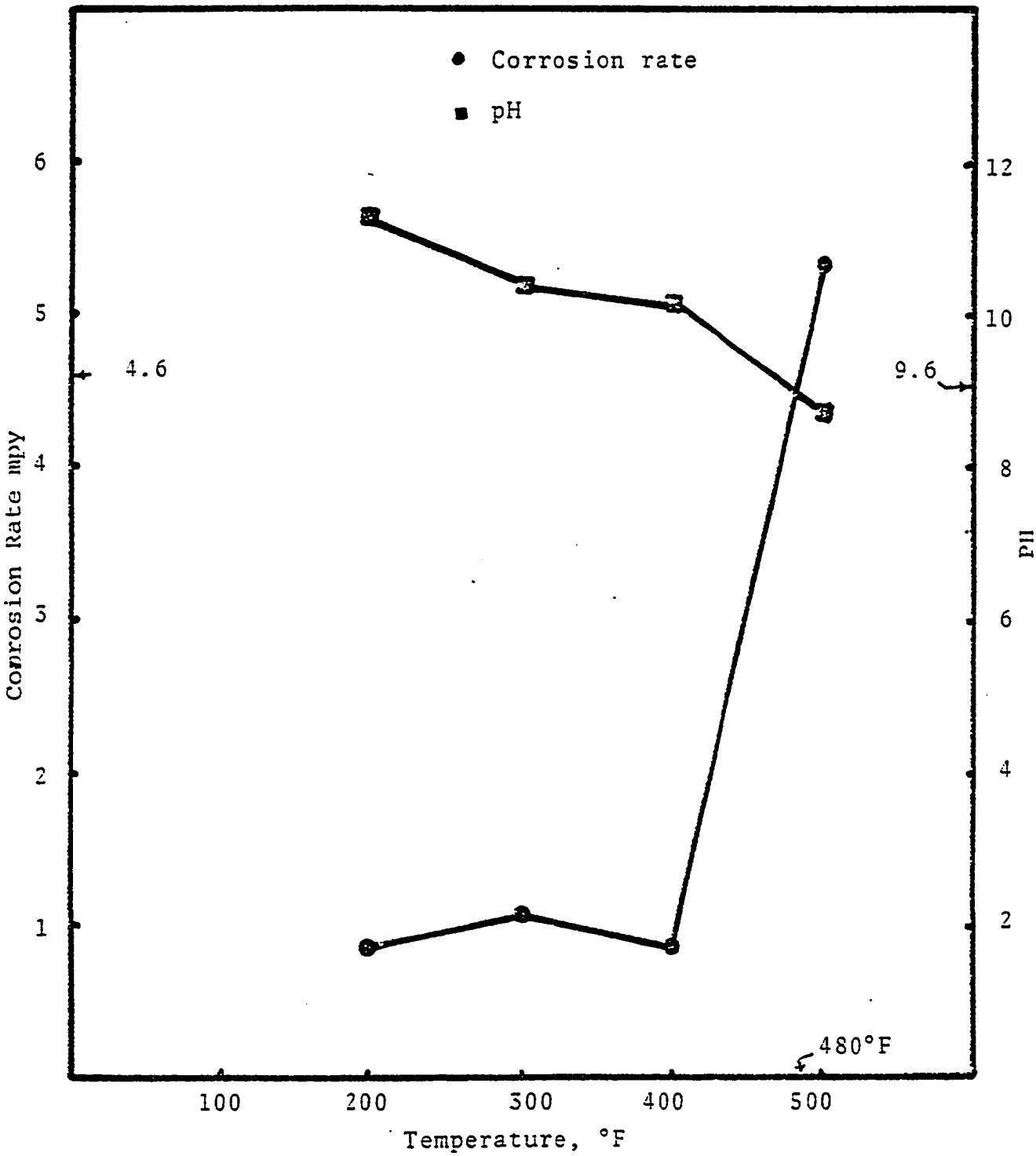


Figure 21: Corrosion rate vs. temperature and pH for Mud B_2

Table 29

Static Test: Mud Type B_2

Room Temp. 84.0°F, 200°F, and 300°F

Test Number	Test Temp °F	pH	Specimen	Mud Weight PPB	Area in^2	Weight Before gram	Weight After gram	Weight Loss mg	Time of Exposure hrs	Corrosion Rate mpy	Average Corrosion Rate mpy
33-1	84 (R.T.)	9.45	ASB21	404.8	2.2422	8.6260	8.6210	5	672	0.226	0.244
			ASB22	404.8	2.530	9.8390	9.8325	6.5	672	0.261	
33-2	200	9.51	ASB21	404.8	2.2422	8.6150	8.606	9.0	72	3.809	2.467
			ASB22	404.8	2.530	9.8140	9.8110	3.0	72	1.125	
33-3	300	9.65	ASB21	404.8	2.2422	8.6060	8.6060	0	42	0	0.311
			ASB22	404.8	2.530	9.8110	9.810	1	42	0.623	

Mud B_3, Group I

Formulation:

80 grams	Resinex
30 grams	Bentonite
30 grams	Sepiolite
10 grams	Sea Salt
10 grams	Caustic Soda
1000 cc	Tap water

Physical Properties from Baroid Rheometer:

Mud Weight	406.8 lb/bbl
pH	11.11
Plastic viscosity	8 cp
Yield Point	12 lb/100 ft^2
Gel, initial	5 lb/100 ft^2
Gel, 10 minutes	25/12

Test temperature was about 200°F after 24 hours rolling test.

Table 30: Corrosion Test

Rolling Test (Temperature 200°F)

C-RB3-200

1	2	3	4	5	6	7	8	9	10	11	12
Test Number	Cell	Specimen	pH	Mud Weight PPB	Area in^2	Coupon Weight Before gram	Coupon Weight After gram	Weight Loss mg	Time of Exposure hrs.	Corrosion Rate mpy	Average Corrosion Rate mpy
33	C	R_1	11.11	406.58	2.53	9.6095	9.6082	1.3	14.5	0.421	2.048
	C	R_2	11.11	406.58	2.53	9.6860	9.6851	0.9	14.5	1.676	negligible

Table 31: Corrosion Test

Rolling Test (Temperature 300°F)

C-RB3-300

34	C	R_1	11.12	406.58	2.53	9.6082	9.6031	5.1	24	5.739	6.302
	C	R_2	11.12	406.58	2.53	9.6851	9.6790	6.1	24	6.865	negligible

Table 32: Corrosion Test

Rolling Test (Temperature 400°F)

C-RB3-400

1	2	3	4	5	6	7	8	9	10	11	12
Test Number	Cell	Specimen	pH	Mud Weight PPB	Area in^2	Coupon Weight Before gram	Coupon Weight After gram	Weight Loss mg	Time of Exposure hrs	Corrosion Rate mpy	Average Corrosion Rate mpy
35	C	R_1	11.12	406.58	2.53	9.6031	9.5940	9.1	24	10.240	9.621
	C	R_2	11.12	406.58	2.53	9.6790	9.6710	8.0	24	9.003	

Table 33: Corrosion Test

Rolling Test (Temperature 500°F)

C-RB3-500

36	C	R_1	9.05	406.58	2.53	9.5940	9.5775	16.5	23	19.375	19.199
	C	R_2	9.05	406.58	2.53	9.6710	9.6548	16.2	23	19.023	

Mud B_3

Corrosion Test: Rolling Technique

Temperature, °F (200, 300, 400, 500)

Table of Results

Temperature °F	pH	Corrosion Rate mpy
200	11.11	2.048
300	11.12	6.302
400	11.12	9.621
500	9.05	19.199

Drilling Fluid B_3

Mud Weight: 406.8 ppg

Temperature °F	pH	Av. Cor. Rate mpy
200	11.11	2.048
300	11.12	6.302
400	11.12	9.621
500	9.05	19.198

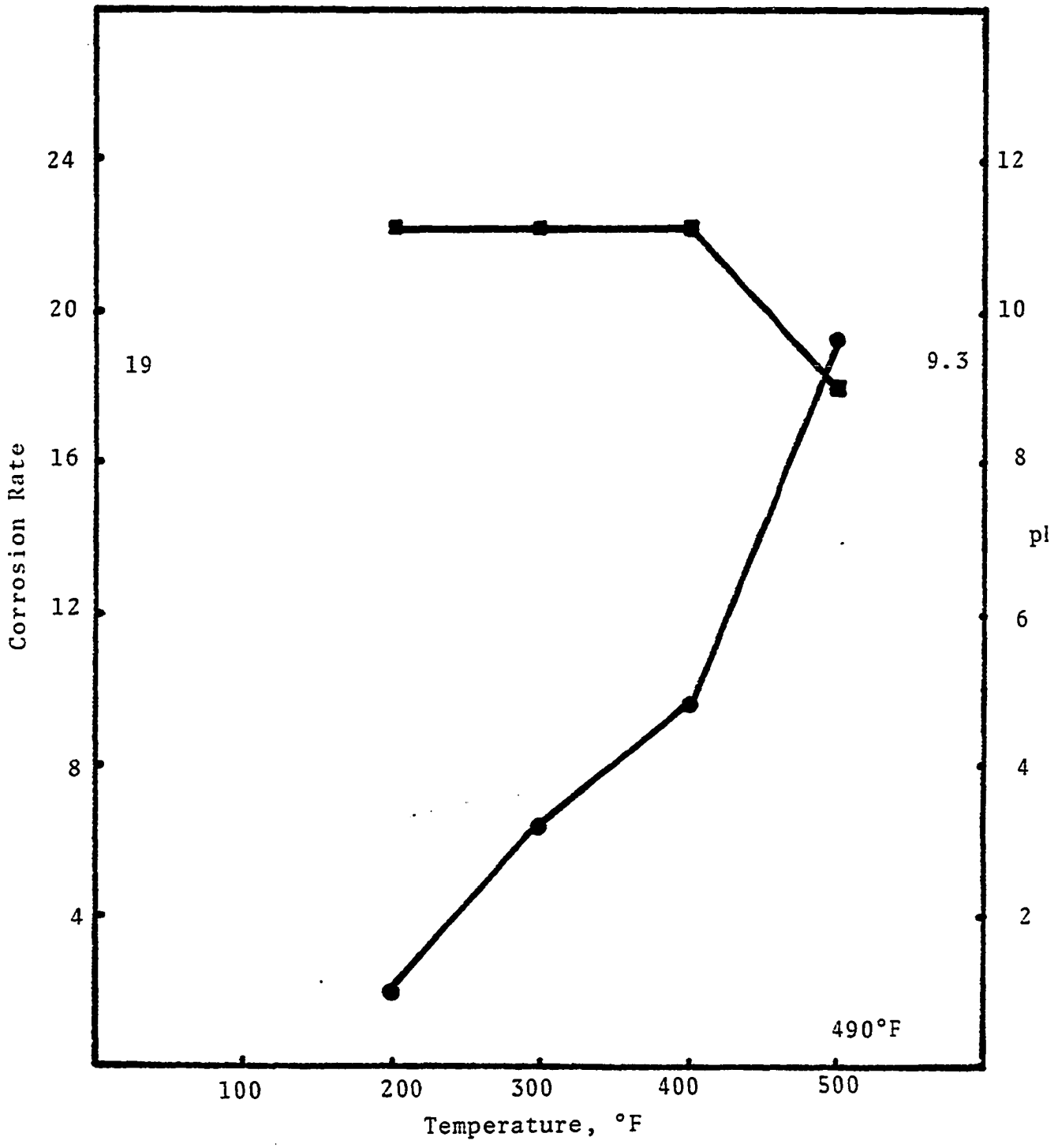


Figure 22: Corrosion rate vs. temperature and pH for mud B_3

Fig. 22

Mud Type B_3, Group III

Formulation:

300 grams	Bentonite clay
300 grams	Sepiolite clay
800 grams	Resinex
100 grams	Sea salt
1000 cc	Tap water

Initial Mud Characteristics:

Mud Weight	406.58 ppb
pH	7.43 (Orion digital pH meter)
Plastic viscosity	8 cp (Baroid rheometer)
Yield	6 lb/100 ft^2
Flow rate	2.262 cc/sec (room temperature)

Table 34: Stabilization Test

Sandia-Lab Flow Loop

Type of Mud: B_3; Mud Weight: 406.58 PPB

Test Number	Time	Temp °F	Line Pressure in/out, psi	pH	Flow Rate cc/sec	Baroid Rheometer ϕ_{600}	Baroid Rheometer ϕ_{300}	Baroid Rheometer Initial Gel lb/100 ft^2	Baroid Rheometer PV cp	Baroid Rheometer YP lb/100 ft^2	Comments
1	11:00	R.T.	1600/1370	7.05	--	--	--	--	--	--	(1)
2	11:30	R.T.	1600/1320	7.43	2.262	22	14	9/5	8	6	
3	12:00	200	1700/1440	7.42	2.083	--	--	--	--	--	(2)
4	1:25	200	1420/1200	7.42	1.920	10	6	3	4	2	
5	2:00	200	1500/1330	7.40	3.169	15	10	4	5	5	
6	2:08	300	1500/1320	7.39	--	--	--	--	--	--	(3)
7	2:20	300	1700/1470	7.30	3.023	14	9	2.5	5	4	
8	2:45	300	1620/1470	7.17		15	10	3	5	5	
9	3:00	400	1440/1200	7.15	3.782	13	8	3	5	3	
10	3:20	400	1700/1440	7.15	3.587	13	8	3	5	3	
	4:00	450	1600/1380	7.13							(4)

(1) Circulating water

(2) Temperature raised to 200°F

(3) Temperature raised to 300°F

(4) Thermal cracking of the 1/4" tubing and steam leak; system shut off

Table 35 .

Corrosion Test: Sandia-Lab Flow Loop

Mud B_3

1	2	3	4	5	6	7	8	9	10	11	12
Test Number	Loop End	Specimen	pH	Mud Weight PPB	Area in^2	Coupon Weight Before gram	Coupon Weight After gram	Weight Loss mg	Time of Exposure hrs	Corrosion Rate mpy	Average Corrosion Rate mpy
38	Hot	MHLB31	7.13/ 7.43*	406.58	2.562	9.7830	9.7650	18.0	5.25	91.442	92.748
	Hot	MHLB32	7.13/ 7.43	406.58	2.562	9.717	9.6985	18.5	5.25	94.005	
39	Hot	HLB31	7.13 7.43	406.58	2.562	9.7885	9.7740	14.5	5.25	73.662	81.282
	Hot	HLB32	7.13/ 7.43	406.58	2.562	9.7625	9.7450	17.5	5.25	88.902	
40	Cold	CLB31	7.13/ 7.43	406.58	2.562	9.6965	9.6920	4.5	5.25	22.860	35.561
	Cold	CLB32	7.13/ 7.43	406.58	2.652	9.6915	9.6820	9.5	5.25	48.26	

Remarks on the Test:

1. The drilling fluid had no caustic soda and pH value started with 7.43 and apparently with temperature, the pH is decreased.

2. The corrosion rate increased with temperature from 35.561 mpy at room temperature (100°F) to 81.282 at the hot end, vertical flow. However, it is higher (91.442) in the mag-corrosion cell in which the two types of flow (vertical and rotational) were eventually combined. The test temperature was raised from room temperature to 450°F (200, 300, 400°F) in 5 hours and 25 minutes, which was the total test duration.

Table 36

Rheological Data with Temperature

Temperature °F	Flow Rate cc/sec	Pressure In/Out psi	P.V. cp	No. of Tests
R.T.	2.262	1600/1300	8	1
200	2.057	1580/1323	4.5	3
300	3.023	1660/1470	5	3
400	3.684	1570/1320	5	2

Corrosion Data

Flow Loop:

a. Hot End:

(i) Mag-Corrosion Cell, average corrosion rate = 92.748 mpy

(ii) Linear Corrosion Cell, average corrosion rate = 81.282 mpy

b. Cold End:

Linear Corrosion Cell, average corrosion rate = 35.561 mpy

Rolling:

At the same conditions of temperature as that of the flow loop, the average corrosion rate =

The test temperature and time of exposure:

Temperature, °F	R.T.	200	300	400	450
Time, hrs	1.0	2.0	3/4	1.0	1/2

Total time of exposure = 5.25 hrs

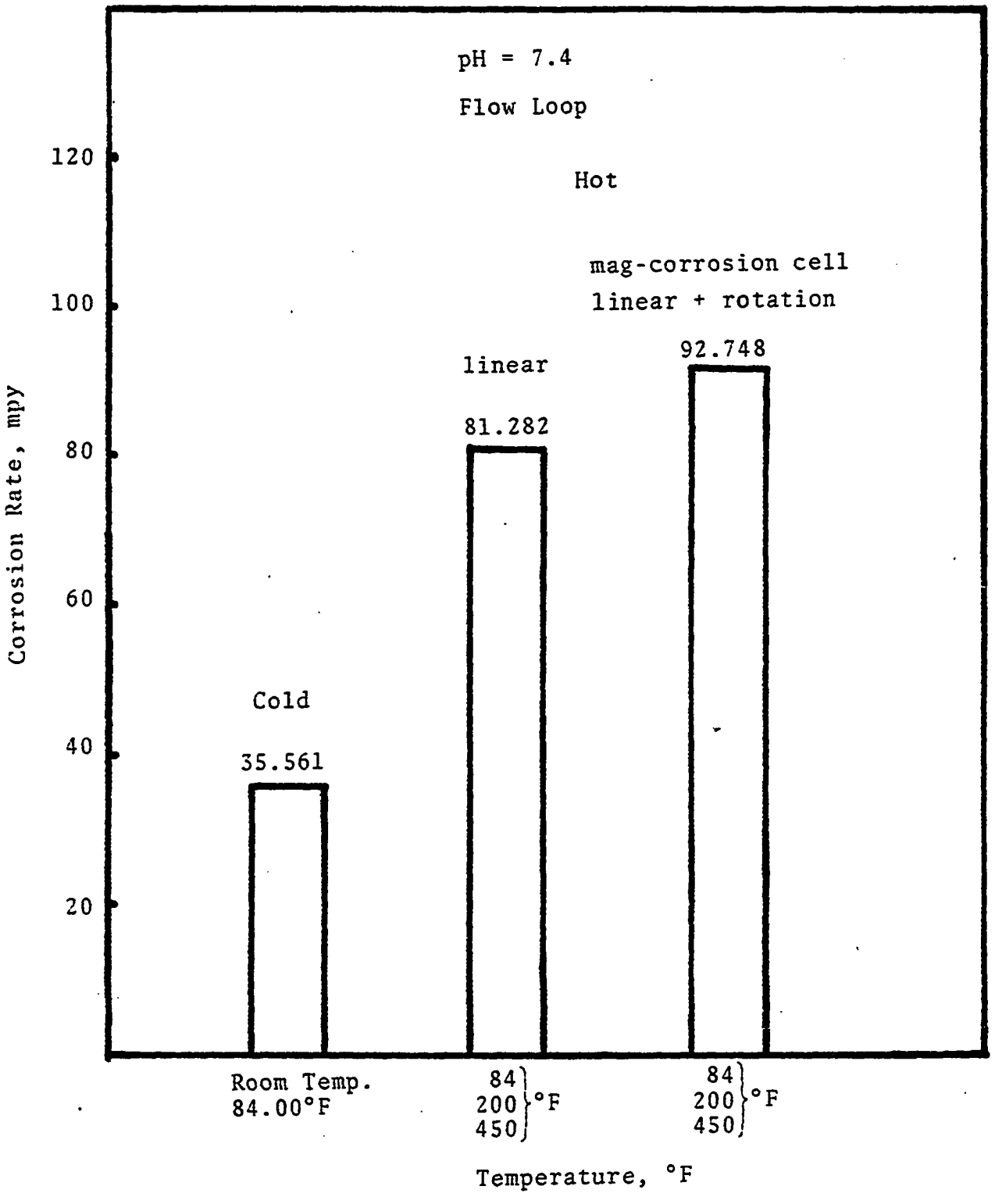


Figure 23: Corrosion rate measured by the flow loop
1% sea salt (cold, hot/linear, hot mag)

Mud Type B_3, Group III

Formulation:

300 grams	Bentonite clay
300 grams	Sepiolite clay
800 grams	Resinex
150 grams	Sea salt
20 grams	Caustic Soda
1000 cc	Tap water

Initial Mud Characteristics:

Mud Weight	8.94 ppg (Mud weight balance)
Plastic viscosity	4 cp (Baroid rheometer)
Yield Point	7 lb/100 ft^2
pH	8.53 (Orion digital pH meter)
Flow Rate	10.204 cc/sec at room temperature

Table 37: Stabilization Test

Sandia-Lab Flow Loop Test 41

Type of Mud: B_3

Test Number	Time	Temp °F	Line Pressure in/out, psi	pH	Flow Rate cc/sec	Baroid Rheometer ϕ_{600}	ϕ_{300}	Initial Gel lb/100 ft^2	PB cp	YP lb/100 ft^2	Comments
1	1:40	R.T.	1600/1300	8.53	10.20	17	12	4.0	4	7	
2	2:00	R.T.	1600/1300	8.48	10.64	--	--	--	--	--	
3	2:30	200	1600/1300	8.48	10.59	--	--	--	--	--	(1)
4	2:45	200	1500/1230	8.47	10.55	15	10	3.5	5	5	(2)
5	3:10	200	1500/1230	8.34	10.55	11.5	10	3.5	4.5	5.5	(3)
6	3:25	200	1500/1240	10.61	10.16	14	9	3	5	4	
7	3:45	200	1460/1200	10.58	10.29	17	11	3.5	6	5	
8	4:05	200	1350/1050	10.56	10.37	18	12	3.5	6	6	
9	4:15	300	1400/1100	10.49	10.8	20	14	6/10	6	8	
10	4:30	300	1400/1100	10.35	10.73	24.5	19	14/20	5.5	14	
11	4:45	300	1500/1100	10.03	10.46	--	--	--	--	--	
12	5:00	300	1300/1100	9.54	10.42	33	29	18	4	25	
13	5:10	300	1200/950	9.06	9.62	34	28	19/25	6	22	
14	5:15	400	1200/970	9.31	7.58	--	--	--	--	--	
15	5:30	400	1400/1100	10.39	7.81	67	60	17	7	53	
16	5:50	400	1300/1000	10.40	7.76	65	58	15	7	51	

(1) Immediately after the system is shut off at temperature 430°F, fresh water is circulated in the loop to (1) displace the drilling fluid left in the flow loop, (2) to clean the flow lines and (3) to cool off the system to room temperature.

(2) The pressure in the lines is maintained between 1500-1600 psi above the vapor pressure to avoid transferring the liquid to vapor phase. Only two or three times, the pressure dropped down to 1200 and 1300 due to some problem with the check valves of the pump.

(3) Concentrated caustic soda is added to the system for two reasons: (1) to maintain the pH value constant and (2) to change the pH from 8 to 10 at 200°F to examine its effect on the plastic viscosity and yield point.

Table 38

Corrosion Test: Sandia-Lab Flow Loop

Mud B_3

1	2	3	4	5	6	7	8	9	10	11	12
Test Number	Loop End	Specimen	pH	Mud Weight PPB	Area in^2	Coupon Weight Before gram	Coupon Weight After gram	Weight Loss mg	Time of Exposure hrs	Corrosion Rate mpy	Average Corrosion Rate mpy
42	Hot	MHLB31	8.34/ 10.61	8.94	2.562	9.7665	9.7600	6.5	5.0	34.672	38.672
	Hot	MHLB32	8.34/ 10.61	8.94	2.562	9.6980	9.6900	8.0	5.0	42.673	
43	Hot	HLB31	8.34/ 10.61	8.94	2.562	9.7740	9.7680	6.0	5.0	32.00	30.669
	Hot	HLB32	8.34/ 10.61	8.94	2.562	9.7450	9.7395	5.5	5.0	29.338	
44	Cold	CLB31	8.34/ 10.61	8.94	2.562	9.6740	9.6700	4.0	5.0	21.336	25.337
	Cold	CLB32	8.34/ 10.61	8.94	2.562	9.6680	9.6635	5.5	5.0	29.338	

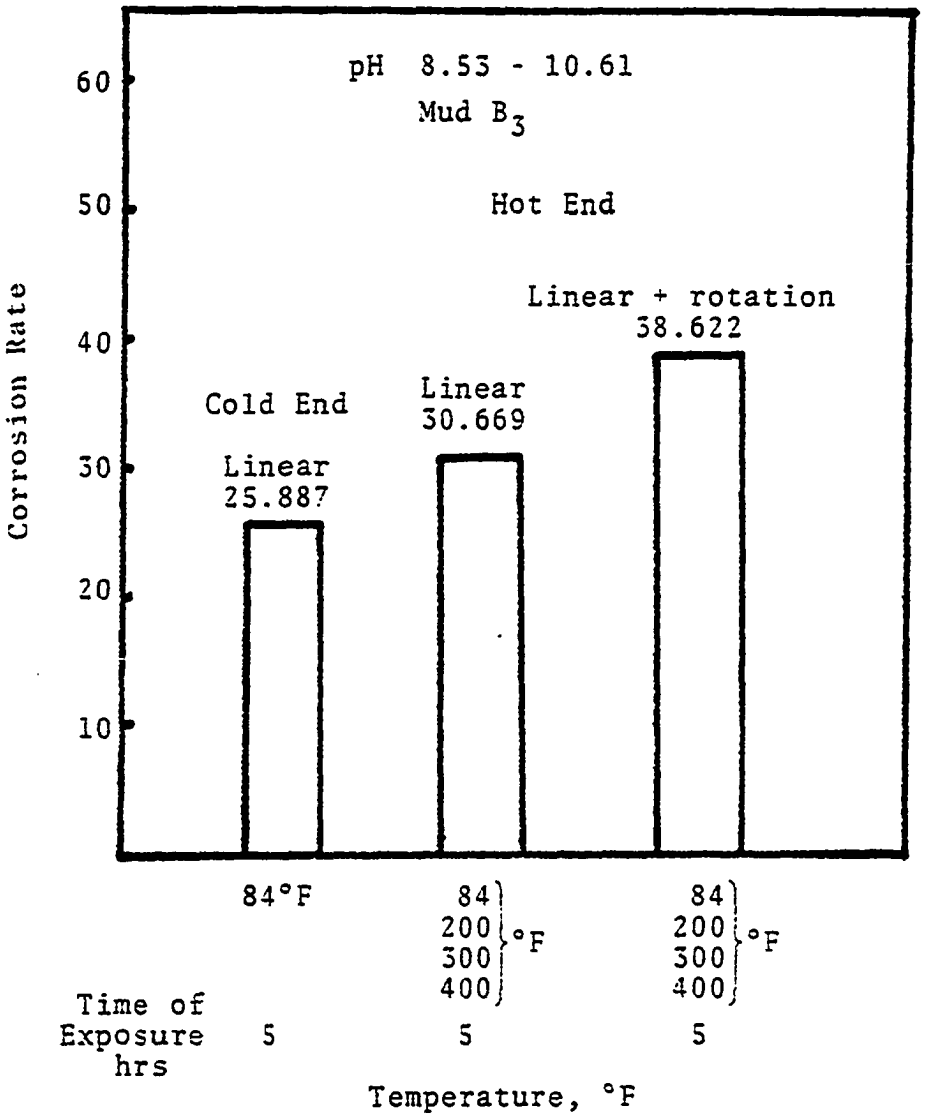


Figure 24: Corrosion rate for different types of flow.

Table 39

Stabilization Test: PGE Flow Loop

Mud Type: Baroid; Mud Weight: 8.84 ppg

Test Number	Time	Temp °F	Line Pressure in/out, psi	pH	Flow Rate cc/sec	Baroid Rheometer ϕ_{600}	ϕ_{300}	Initial Gel lb/100 ft^2	PV cp	YP lb/100 ft^2	Δp 3/8" psi	Δp 1/4" psi
1	10:00	R.T.	600/410	10.8	3.82						1.30	0.29
2	10:35	R.T.	500	11.00	4.1						1.39	0.28
3	10:45	R.T.	500	11.12	4.66						1.32	0.26
4	11:00	R.T.	490	11.14	4.56						1.30	0.27
5	11:20	T.T.	500	11.13	4.62	8	3.5	2	4.5	1	1.31	0.28
6	11:40	200	500	11.12	4.52						1.20	0.24
7	12:10	200	550	11.02	4.57						1.21	0.26
8	12:50	200	480	10.96	4.61	8	3.5	2	4.5	1	1.20	0.24
9	1:25	300	400	10.85	4.70						1.18	0.25
10	1:45	300	450	10.72	4.87						1.17	0.27
11	2:05	300	475	10.69	4.86	7.5	3.5	1.5	4	0.5	1.20	0.29

Corrosion Data

Flow Loop:

a. Hot End

(i) Mag-Corrosion Cell, average corrosion rate = 38.622 mpy

(ii) Linear Corrosion Cell, average corrosion rate = 30.669 mpy

b. Cold End

Linear Corrosion Cell, average corrosion rate = 25.337 mpy

APPENDIX C

SET-UP PHOTOGRAPHS

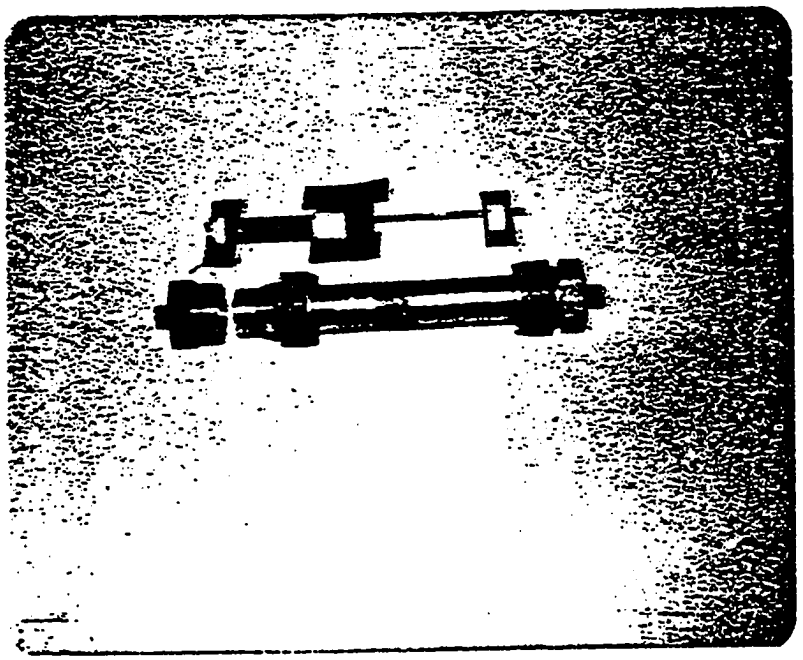


Figure 25: View of the linear corrosion cell in parts loaded with the specimen

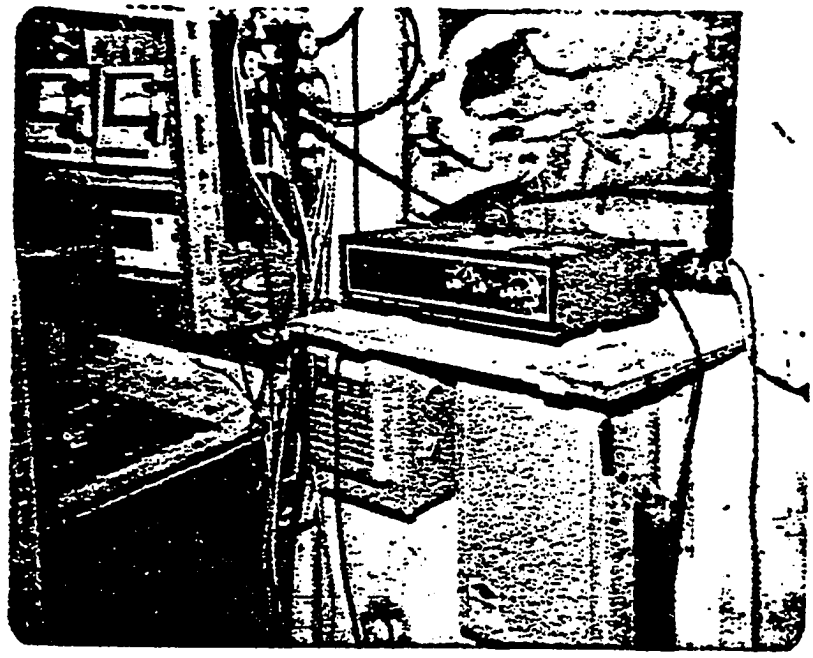


Figure 26: View of the flow loop, pH meter, transducers and power switch.

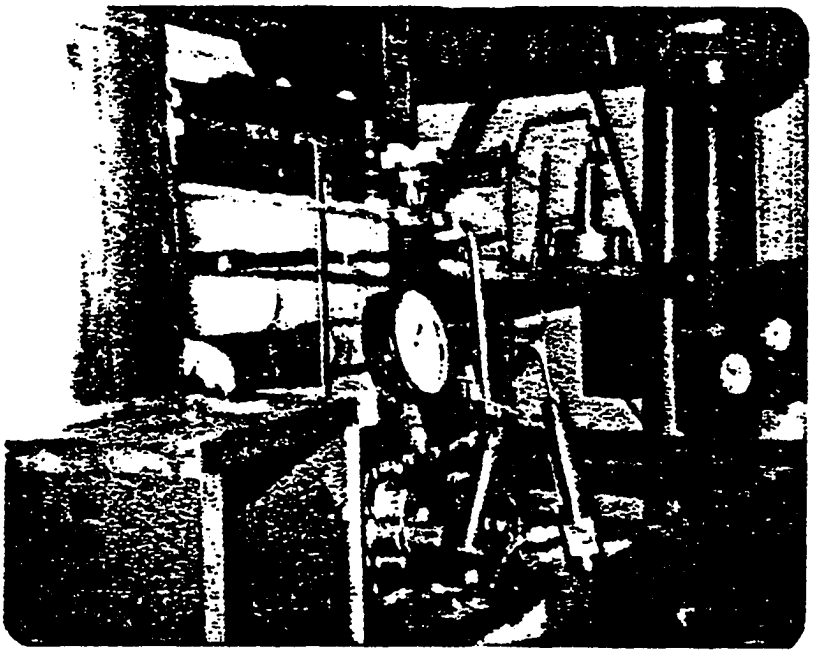


Figure 27: View of the two shear valves installed in series with the cold end of the loop.

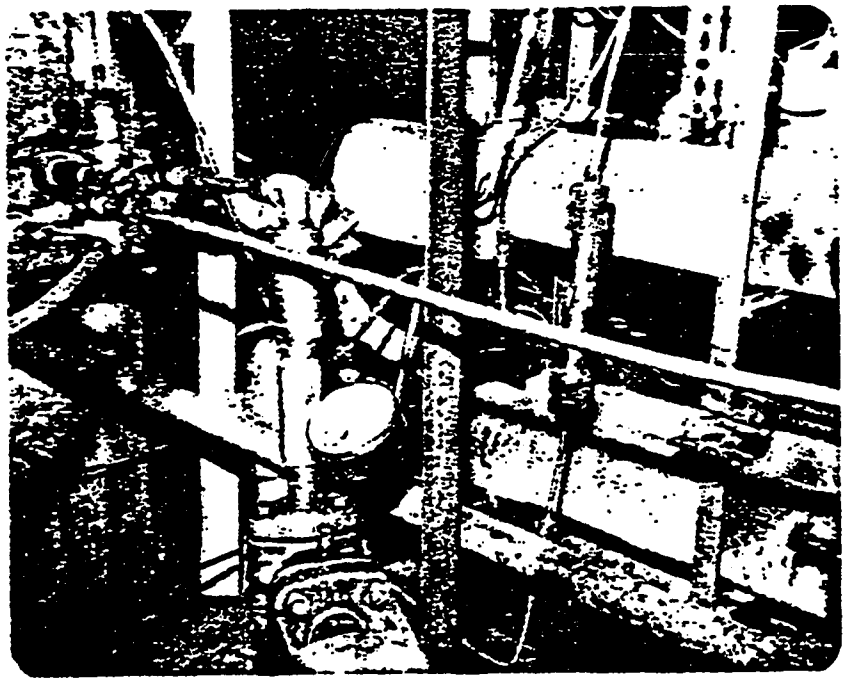


Figure 28: View of the linear corrosion cell attached to the cold end of the flow loop.

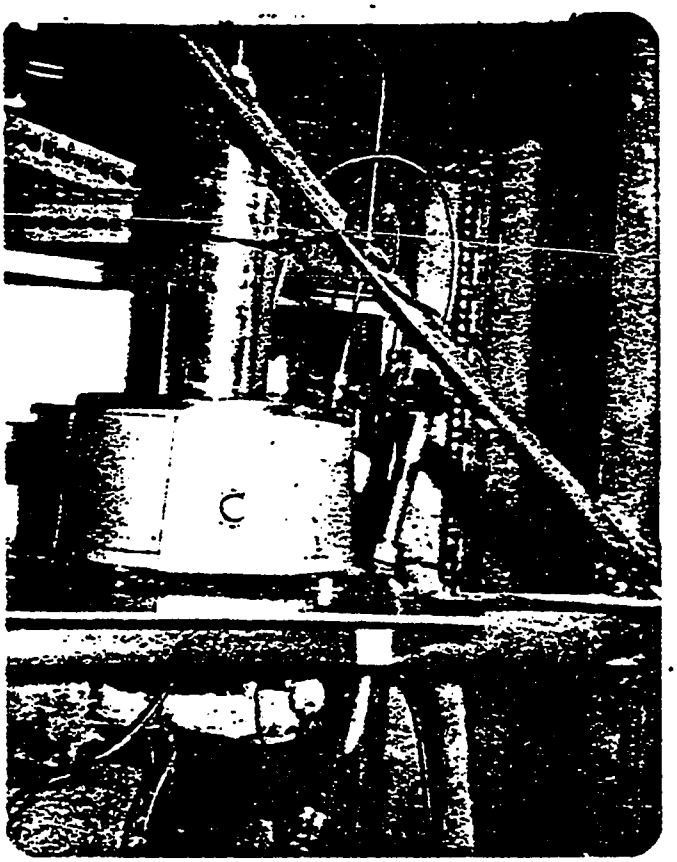


Figure 29: View of the mag-corrosion and the linear cells attached to the hot end of the loop.



Figure 30: Steam leak due to thermal cracking of one of the flow lines.